Supporting Information

"Flagellate Effect" of Thermally Activated Delayed Fluorescence Emitter Dominating the Efficiency of Non-doped Solution Processable OLEDs

Guimin Zhao, Yuheng Lou, Renjie Ji, Qiyin Ran, Haowen Chen, Wenwen Tian, Wei Jiang, Yueming Sun*

Jiangsu Province Hi-Tech Key Laboratory for Bio-Medical Research, Jiangsu Engineering Laboratory of Smart Carbon-Rich Materials and Device, School of Chemistry and Chemical Engineering, Southeast University, Nanjing, Jiangsu, 211189, China.

*Corresponding author:

E-mail addresses: jiangw@seu.edu.cn (W. Jiang).

1. General Information

1.1 Materials and measurements

All reagents were purchased from commercial sources and used directly without further purification. The reactions used were carried out under nitrogen protection. ^{1}H spectra and ^{13}C spectra were recorded on a Bruker Dex-600/150 NMR spectrometers in $CDCl_3$ solution. Molecular weights of the dendrimers were tested by matrix assisted laser desorption-ionization time-of-flight mass spectrometry (MALDI-TOF-MS) using a BRUKER DALTONICS instrument, with α-cyano-hydroxycinnamic acid as a matrix. Elemental analysis was determined by an Elementar Vario EL CHN elemental analyzer. UV-Vis spectra were recorded on a SHIMADZU UV-2450 spectrophotometer. The photoluminescence (PL) spectra were measured on a HORIBA FLUOROMAX-4 spectrophotometer at room temperature (excitation wavelength of 350 nm). The low-temperature phosphorescence (PH) spectra were recorded on F-7000 FL spectrophotometer in toluene solution (10^{-5} M) by setting delay time (100 μs) and liquid nitrogen (77 K, excitation wavelength of 325 nm). The transient PL decay curves of solution and film samples were obtained by EDIBURGH FLS-1000 instruments (375 nm laser). And the solid PL quantum efficiency was measured using an integrating sphere under an excitation wavelength of 350 nm. Cyclic voltammetry was performed using a CHI750C voltammetric analyzer with a scan rate of 100 mV/s at room temperature to investigate the oxidation potentials. A traditional three electrode cell was used as electrolytic cell, in which tetra-n-butylammonium hexafluorophosphate (Bu_4NPF_6) dissolving in dry CH_2Cl_2 solution (10^{-3} M) was employed as electrolyte. Platinum disk is used as the working electrode, platinum wire is regarded as the counter electrode and silver wire is used as the reference electrode. Ferrocenium/ferrocene (Fc/Fc^{+}) is used as the external standard compound. The HOMO and LUMO levels were calculated according to the equations E_{HOMO} = -e ($E_{onset,\ ox}$ + 4.4 V), $E_{LUMO} = E_{HOMO} + E_g$, where $E_{onset,\ ox}$ is the onset value of the first oxidation wave and E_g is the optical bandgap estimated from the absorption onset. Thermogravimetric analysis (TGA) and differential scanning calorimetry (DSC) curves were performed with a Netzsch simultaneous thermal analyzer system (STA 409 PC) from 20 °C to 800 °C and DSC 2910 modulated calorimeter from 20 °C to 200 °C at a 10 °C/min heating rate under N_2 atmosphere, respectively. AFM measurements were obtained by using a Seiko instrument, SPA-400 in a tapping mode (5 × 5 μm^2)

to study the surface morphology of emission layers.

1.2 Theoretical computation method

The theoretical calculation was carried out with the Gaussian 09 software package. Geometry optimizations were conducted under the B3LYP/6-31G(d) level of theory. The ground state geometries were optimized by density functional theory (DFT) at the B3LYP functional. In order to investigate the transition energies and the transition characters of the lowest excited singlet (S_1) and triplet states (T_1), time-dependent density functional theory (TD-DFT) method with B3LYP level, was carried out to calculate the energies of S_1, T_1, and singlet-triplet splitting energy (ΔE_{ST}). For investigating the properties of excited-states, natural transition orbitals (NTOs) were evaluated for the ten lowest excited-states, involving both singlet and triplet states under B3LYP/6-31G(d) level. The corresponding visualization of images for these theoretical computations were exported by Multiwfn 3.7 software.[1] The 10-ns molecular dynamics (MD) simulation was performed with GROMACS software package (version 2019.3) using general Amber force field (GAFF) and restrained electrostatic potential (RESP) atomic charge, which was visualized by VMD program.[2, 3] Firstly, Gaussian optimized ground state configuration is used as input file, and 50 molecules were randomly placed into a cubic simulation box with an initially size of 10×10×10 nm^3. The fastest descent method is used to minimize the energy. In order to pre-balance the structure, 1 ns NVT at T = 300 K and 1 ns NPT at T = 300 K, P = 1 bar were successively performed. Finally, 10 ns dynamic simulation was performed for the balanced structure at T = 300 K, P = 1 bar. In order to exclude the boundary effect, three-dimensional periodic boundary conditions (PBC) are used. At the end of the operation, the inner layer molecules were taken to analyze the flexible chain stretching and stacking, and the extracted energy was mapped and calculated.

1.3 Device preparation process

OLED devices were fabricated using a clean glass substrate coated with an ITO layer as the anode, with a sheet resistance of 15 Ω cm^{-2} and an active pattern size of 2 × 2 mm^2. Before device fabrication, the glass substrates were sequentially cleaned in an ultrasonic bath with deionized water, acetone and ethanol for three times, and then the ITO substrate was treated with UV-ozone for 30 minutes. The OLED configuration was as follows: ITO/PEDOT:PSS (40 nm)/EML(40 nm)/POT2T (30 nm)/Cs_2CO_3 (1 nm)/Al (100 nm), where PEDOT:PSS and Cs_2CO_3 acted as the hole and electron

injection layers, respectively. The POT2T and Al functioned as the electron transport layers and the cathode, respectively. The PEDOT:PSS was directly spin-coated on an ITO plate and annealed at 150 °C for 10 min. The EML was dissolved in 1, 2-dichloroethane (10 mg mL^{-1}), then spin-coated and annealed at 80 °C for 10 min under nitrogen atmosphere. Subsequently, a 30 nm thick PO-T2T was spin-coated from isopropanol solution as the electron transporting layer (ETL). The ETL was baked and annealed at 80 ℃ for 10 min under N_2 atmosphere. Then, the substrates were moved into a vacuum chamber to deposit Cs_2CO_3 (1 nm), and Al (100 nm) sequentially using a thermal evaporator. The current density-voltage-luminance characteristics, current efficiency and power efficiency were tested using a Keithley 2400 Sourcemeter coupled with Si-potodiodes calibrated with PR655. The EL spectra were collected with a Photo-Research PR655 SpectraScan. All the characterizations were performed at room temperature in ambient condition without encapsulation. External quantum efficiencies of the devices were calculated assuming a Lambertian emission distribution. The carrier-only devices were fabricated with a structure of ITO |Al (50 nm) |EML (40 nm) |POT2T (30 nm) |Cs_2CO_3 (1 nm) |Al (100 nm) for electron-only device, and a configuration of ITO |PEDOT:PSS (40 nm) |EML (40 nm) |MoO_3 (20 nm) |Al (100 nm) for hole-only devices.

1.4 Calculation of rate constants

$$k_{r,S} = \frac{\Phi_p}{\tau_p} \quad (1)$$

$$k_{ISC} = k_p\left(1 - \Phi_p\right) \quad (2)$$

$$k_{RISC} = \frac{\Phi_d \, k_d k_p}{k_{ISC}\Phi_p} \quad (3)$$

$$k_{nr,T} = k_d - \Phi_p k_{RISC} \quad (4)$$

$$\Phi_p = \frac{A_1\tau_p}{A_1\tau_p + A_2\tau_d}\Phi_{PL} \quad (5)$$

$$\Phi_d = \frac{A_2\tau_d}{A_1\tau_p + A_2\tau_d}\Phi_{PL} \quad (6)$$

$$k_p = {}^{1}/_{\tau_p} \quad (7)$$

$$k_d = {}^{1}/_{\tau_d} \quad (8)$$

The rate constants can be calculated according to above equation (1)-(6): Where τ_p and τ_d are the prompt and delayed lifetime respectively. Φ_{PL}, Φ_P and Φ_d are the total PL quantum yield, prompt fluorescence and delayed fluorescence quantum yield, respectively. $k_{r,S}$, $k_{nr,T}$, k_{ISC} and

k_{RISC} are the rate constant for fluorescence radiative transition of singlet exciton, non-radiative transition of triplet exciton, intersystem crossing (ISC) and reverse intersystem crossing (RISC) processes, respectively. A_1 and A_2 are the frequency factors according to the followed fitting model of transient PL decay curves: $I(t) = A_1 \exp\left(-\frac{t_1}{\tau_p}\right) + A_2 \exp\left(-\frac{t_2}{\tau_d}\right)$.[4]

2. Synthetic Procedures and Characterized Data

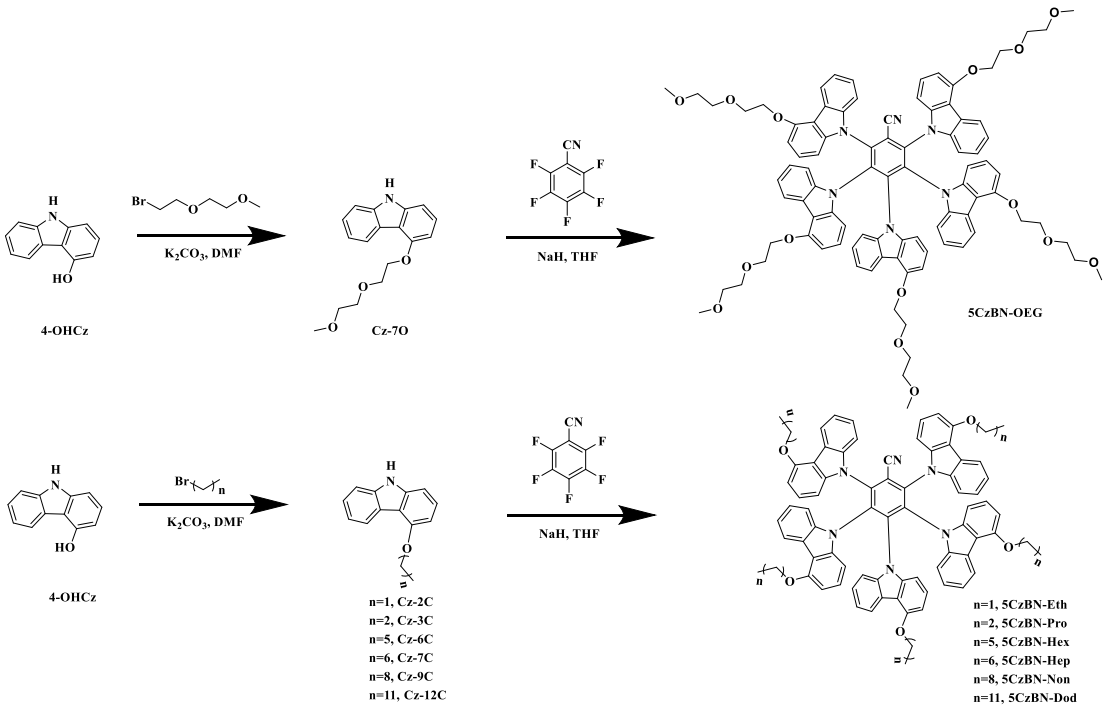

Scheme S1. Synthetic pathways toward molecules 5CzBN-Eth, 5CzBN-Pro, 5CzBN-Hex, 5CzBN-Hep, 5CzBN-OEG, 5CzBN-Non and 5CzBN-Dod.

The molecule 5CzBN-Hex were obtained according to the reported reference.[5]

The synthesis of 3-ethoxy-9H-carbazole (Cz-2C)

A mixture of 9H-carbazol-4-ol (1 g, 5.46 mmol), 1-bromoethane (0.7 g, 6.42 mmol) and potassium carbonate (K_2CO_3, 2.26 g, 16.38 mmol) was added to 20 mL N, N-dimethylformamide (DMF). The reaction taken place at room temperature under nitrogen for 4 hours. After completion, the mixture was poured into 100 mL water. The crude product was extracted (ethyl acetate: petroleum ether), and purified by silica gel column chromatography to give the white powder (0.92 g, 80%). ^{1}H NMR (600 MHz, $CDCl_3$): δ = 8.28 (d, J=7.8 Hz, 1H), 7.94 (s, 1H), 7.32 (d, J=3.9 Hz, 2H), 7.26 (t, J=8.0 Hz, 1H), 6.95 (d, J=8.0 Hz, 1H), 6.60 (d, J=7.9 Hz, 1H), 4.23 (d, J=7.0 Hz, 2H), 1.55 (t, J=7.0 Hz, 3H). ^{13}C NMR (150 MHz, $CDCl_3$): δ = 155.65, 140.95, 138.72, 126.69, 124.88, 123.10, 122.81,

119.58, 112.70, 109.90, 103.30, 101.16, 63.61, 15.09.

The synthesis of 3-propoxy-9H-carbazole (Cz-3C)

The synthetic route of Cz-3C was akin to that of Cz-2C, when the 1-bromoethane was replaced with 1-bromopropane. Similarly, the white product was obtained with a high yield (1.05 g, 85%). ^{1}H NMR (600 MHz, $CDCl_3$): δ = 8.28 (d, J=7.7 Hz, 1H), 7.98 (s, 1H), 7.39-7.30 (m, 2H), 7.27 (t, J=8.0 Hz, 1H), 6.97 (d, J=8.0 Hz, 1H), 6.62 (d, J=7.9 Hz, 1H), 4.15 (t, J=6.3 Hz, 2H), 1.97 (m, 2H), 1.15 (t, J=7.4 Hz, 3H). ^{13}C NMR (150 MHz, $CDCl_3$): δ =155.80, 140.94, 138.71, 126.70, 124.85, 123.08, 122.85, 119.60, 112.74, 109.89, 103.23, 101.09, 69.53, 22.88, 10.94.

The synthesis of 3-(heptyloxy)-9H-carbazole (Cz-7C)

The synthetic route of Cz-7C was akin to that of Cz-2C, when the 1-bromoethane was replaced with 1-bromoheptane. Similarly, the white product was obtained with a high yield (1.31 g, 85%). ^{1}H NMR (600 MHz, $CDCl_3$): δ = 8.26 (d, J=7.8 Hz, 1H), 7.93 (s, 1H), 7.31 (d, J=3.9 Hz, 2H), 7.18 (dd, J=7.4, 4.5 Hz, 1H), 6.94 (d, J=8.0 Hz, 1H), 6.60 (d, J=7.9 Hz, 1H), 4.15 (t, J=6.4 Hz, 2H), 2.00-1.85 (m, 2H), 1.55 (t, J=7.7 Hz, 2H), 1.38 (m, 2H), 1.28 (dd, J=8.9, 5.2 Hz, 4H), 0.85 (t, J=6.9 Hz, 3H). ^{13}C NMR (150 MHz, $CDCl_3$): δ = 155.81, 140.94, 138.71, 126.70, 124.85, 123.09, 122.85, 119.59, 112.72, 109.90, 103.23, 101.08, 68.00, 31.85, 29.52, 29.15, 26.26, 22.67, 14.14.

The synthesis of 3-(2-(2-methoxyethoxy)ethoxy)-9H-carbazole (Cz-7O)

The synthetic route of Cz-7O was akin to that of Cz-2C, when the 1-bromoethane was replaced with 1-bromo-2-(2-methoxyethoxy)ethane. Similarly, the white product was obtained with a high yield (1.37 g, 88%). ^{1}H NMR (600 MHz, $CDCl_3$): δ = 8.35 (d, J=7.7 Hz, 1H), 8.12 (s, 1H), 7.38 (td, J=7.2, 3.7 Hz, 2H), 7.31 (td, J=8.0, 4.3 Hz, 1H), 7.04 (m, 1H), 6.66 (t, J=7.4 Hz, 1H), 4.46-4.30 (m, 2H), 4.07 (dd, J=7.2, 2.7 Hz, 2H), 3.89-3.75 (m, 2H), 3.62 (dt, J=4.1, 2.9 Hz, 2H), 3.42 (d, J=2.6 Hz, 3H). ^{13}C NMR (150 MHz, $CDCl_3$): δ = 155.28, 141.00, 138.78, 126.64, 124.94, 123.17, 122.66, 119.55, 112.81, 110.00, 103.76, 101.30, 72.08, 70.84, 70.00, 67.51, 59.13.

The synthesis of 3-(nonyloxy)-9H-carbazole (Cz-9C)

The synthetic route of Cz-9C was akin to that of Cz-2C, when the 1-bromoethane was replaced with 1-bromononane. Similarly, the white product was obtained with a high yield (1.45 g, 86%). ^{1}H NMR (600 MHz, $CDCl_3$): δ = 8.27 (d, J=7.8 Hz, 1H), 7.96 (s, 1H), 7.36-7.29 (m, 2H), 7.22-7.15 (m, 1H), 6.96 (d, J=8.0 Hz, 1H), 6.61 (d, J=8.0 Hz, 1H), 4.16 (t, J=6.4 Hz, 2H), 2.02-1.85 (m, 2H), 1.56 (m,

2H), 1.41-1.18 (m, 10H), 0.83 (t, J=6.9 Hz, 3H). ^{13}C NMR (150 MHz, $CDCl_3$): δ = 155.81, 140.94, 138.70, 126.68, 124.84, 123.08, 122.85, 119.58, 112.74, 109.87, 103.20, 101.08, 68.00, 31.92, 29.58, 29.50, 29.46, 29.30, 26.28, 22.71, 14.13.

The synthesis of 3-(dodecyloxy)-9H-carbazole (Cz-12C)

The synthetic route of Cz-12C was akin to that of Cz-2C, when the 1-bromoethane was replaced with 1-bromododecane. Similarly, the white product was obtained with a high yield (1.63 g, 85%). ^{1}H NMR (600 MHz, $CDCl_3$): δ = 8.32 (d, J=7.7 Hz, 1H), 7.93 (s, 1H), 7.40-7.32 (m, 2H), 7.23 (dd, J=10.4, 3.7 Hz, 1H), 6.97 (d, J=8.0 Hz, 1H), 6.64 (d, J=8.0 Hz, 1H), 4.20 (t, J=6.4 Hz, 2H), 2.03-1.93 (m, 2H), 1.60 (m, 2H), 1.46-1.21 (m, 16H), 0.88 (t, J=7.0 Hz, 3H). ^{13}C NMR (150 MHz, $CDCl_3$): δ = 155.83, 140.96, 138.73, 126.70, 124.86, 123.10, 122.85, 119.61, 112.74, 109.93, 103.26, 101.10, 68.03, 31.98, 29.75, 29.72, 29.68, 29.67, 29.53, 29.50, 29.42, 26.31, 22.75, 14.18.

The synthesis of (2R,4R)-2,3,4,5,6-pentakis(4-ethoxy-9H-carbazol-9-yl)benzonitrile (5CzBN-Eth)

Under nitrogen atmosphere, Cz-2C (0.9 g, 4.26 mmol) was dissolved to anhydrous DMF (10 mL), and an anhydrous DMF (10 mL) solution containing NaH (0.51 g, 12.78 mmol) was slowly added to the above mixture for 10 min. The mixture was continued to stir for 3 h. Then, 2,3,4,5,6-pentafluorobenzonitrile (0.10 g, 0.53 mmol) in anhydrous DMF (1 mL) was added dropwise for 10 min. Then the solution was stirred for 24 h at room temperature. After completion, 100 mL of water was added into the solution and the mixture was extracted with CH_2Cl_2 for three times. The combined organic layer was dried with anhydrous $MgSO_4$ and the organic solvent was further removed under vacuum. The precipitate was purified by column chromatography on silica gel with the petroleum ether and dichloromethane (v:v=1:1, R_f=0.29), obtaining the bright green-yellow product (0.46 g, 75%). ^{1}H NMR (600 MHz, $CDCl_3$) δ = 8.01 (t, J=7.6 Hz, 2H), 7.59 (m, 3H), 7.24-7.01 (m, 9H), 7.00-6.68 (m, 10H), 6.56 (m, 8H), 6.23-6.11 (m, 3H), 4.11-3.83 (m, 10H), 1.51-1.46 (m, 7H), 1.31-1.26 (m, 8H). ^{13}C NMR (150 MHz, $CDCl_3$) δ = 155.28, 155.23, 154.47, 154.40, 142.07, 140.73, 140.60, 140.53, 139.56, 139.36, 138.43, 138.37, 137.36, 137.19, 126.28, 126.17, 125.07, 124.32, 123.56, 123.30, 123.27, 123.05, 122.26, 121.03, 120.60, 120.44, 117.19, 113.45, 113.12, 112.43, 110.17, 109.81, 109.77, 109.60, 103.90, 103.56, 103.28, 103.19, 103.13, 103.03, 102.90, 63.62, 63.36, 63.30, 14.93, 14.74, 14.69. MS(MALDI-TOF) [m/z]: calcd for $C_{77}H_{60}N_6O_5$,

1149.360; found, 1149.471. Anal. Calcd for $C_{77}H_{60}N_6O_5$: C, 80.47; H, 5.26; N, 7.31. Found: C, 80.44; H, 5.27; N, 7.30.

The synthesis of (2R,4R)-2,3,4,5,6-pentakis(4-propoxy-9H-carbazol-9-yl)benzonitrile (5CzBN-Pro)

The synthetic route of 5CzBN-Pro was similar to that of 5CzBN-Eth, when the Cz-2C was replaced with Cz-3C. Similarly, the precipitate was purified by column chromatography on silica gel with the petroleum ether and dichloromethane (v:v=1:1, R_f=0.30), and the bright green-yellow product was obtained with a considerable yield (70%). ^{1}H NMR (600 MHz, $CDCl_3$) δ = 8.01-7.99 (t, J=8.1 Hz, 2H), 7.60-7.55 (m, 3H), 7.16-7.14 (m, 2H), 7.12-7.01 (m, 6H), 7.00-6.94 (m, 2H), 6.93-6.67 (m, 9H), 6.64-6.48 (m, 8H), 6.25-6.12 (m, 3H), 4.04-4.00 (m, 4H), 3.89-3.70 (m, 6H), 1.90-1.87 (m, 4H), 1.76-1.68 (m, 6H), 1.10-1.08 (m, 6H), 0.98-0.93 (m, 9H). ^{13}C NMR (150 MHz, $CDCl_3$) δ = 155.43, 155.40, 155.38, 154.63, 154.61, 154.57, 154.55, 142.23, 140.76, 140.56, 139.62, 139.45, 138.46, 138.40, 137.43, 137.28, 126.24, 125.07, 124.29, 123.62, 123.28, 123.01, 122.27, 121.05, 120.45, 117.20, 113.53, 113.22, 112.48, 110.20, 109.84, 109.68, 109.62, 103.89, 103.87, 103.54, 103.50, 103.16, 103.11, 102.93, 102.78, 69.56, 69.33, 69.28, 22.71, 22.55, 22.51, 10.83, 10.70, 10.66. MS(MALDI-TOF) [m/z]: calcd for $C_{82}H_{70}N_6O_5$, 1219.500; found, 1219.549. Anal. Calcd for $C_{82}H_{70}N_6O_5$: C, 80.76; H, 5.79; N, 6.89. Found: C, 80.74; H, 5.77; N, 6.90.

The synthesis of (2R,4R)-2,3,4,5,6-pentakis(4-(heptyloxy)-9H-carbazol-9-yl)benzonitrile (5CzBN-Hep)

The synthetic route of 5CzBN-Hep was similar to that of 5CzBN-Eth, when the Cz-2C was replaced with Cz-7C. Similarly, the precipitate was purified by column chromatography on silica gel with the petroleum ether and dichloromethane (v:v=1.5:1, R_f=0.28), and the bright green-yellow product was obtained with a considerable yield (73%). ^{1}H NMR (600 MHz, $CDCl_3$) δ = 8.43-8.42 (d, J=7.4 Hz, 1H), 7.99 (s, 2H), 7.64-7.60 (m, 2H), 7.54-7.53 (d, J=7.0 Hz, 2H), 7.42-7.39 (t, J=7.1 Hz, 1H), 7.24-6.96 (m, 12H), 6.92-6.89 (m, 2H), 6.87 - 6.41 (m, 11H), 6.37-6.11 (m, 2H), 4.27 (dd, J=10.1, 6.1 Hz, 2H), 4.04-4.03 (d, J=5.1 Hz, 5H), 3.86-3.80 (m, 3H), 2.05-2.02 (t, J=9.8 Hz, 2H), 1.90-1.85 (m, 5H), 1.77-1.69 (m, 2H), 1.68-1.62 (m, 2H), 1.51-1.49 (m, 9H), 1.38-1.28 (m, 30H), 0.97-0.81 (m, 15H). ^{13}C NMR (150 MHz, $CDCl_3$) δ = 155.99, 155.87, 155.47, 155.13, 154.74, 141.89, 140.76, 139.76, 138.55, 138.35, 137.55, 136.65, 135.97, 134.66, 127.48, 126.33, 125.53, 125.36, 124.40,

123.80, 123.59, 123.38, 123.24, 123.01, 122.74, 122.34, 121.35, 120.86, 120.38, 117.02, 113.51, 113.12, 112.44, 109.80, 109.57, 109.34, 109.25, 103.23, 102.94, 102.66, 102.49, 70.57, 68.24, 67.98, 67.79, 31.85, 31.81, 31.77, 29.54, 29.37, 29.26, 29.18, 29.12, 29.07, 26.28, 26.15, 26.04, 22.68, 22.63, 14.58, 14.15, 14.11. MS(MALDI-TOF) [m/z]: calcd for $C_{102}H_{110}N_6O_5$, 1498.850; found, 1499.626. Anal. Calcd for $C_{102}H_{110}N_6O_5$: C, 81.67; H, 7.39; N, 5.60. Found: C, 81.70; H, 7.37; N, 5.62.

The synthesis of (2R,4R)-2,3,4,5,6-pentakis(4-(2-(2-methoxyethoxy)ethoxy)-9H-carbazol-9-yl)benzonitrile (5CzBN-OEG)

The synthetic route of O5CzBN-Hep was similar to that of 5CzBN-Eth, when the Cz-2C was replaced with Cz-7O. Similarly, the precipitate was purified by column chromatography on silica gel with the ethyl acetate and dichloromethane (v:v=1:1, R_f=0.25), and the bright yellow product was obtained with a considerable yield (50%). ^{1}H NMR (600 MHz, $CDCl_3$) δ = 8.26-8.24 (m, 2H), 7.89-7.77 (m, 3H), 7.48-7.14 (m, 13H), 7.12-6.93 (m, 7H), 6.87-6.73 (m, 7H), 6.48-6.42 (m, 3H), 4.50-4.48 (m, 4H), 4.33-4.14 (m, 11H), 3.99 (m, 10H), 3.82 (m, 10H), 3.70 (m, 5H), 3.63-3.47 (m, 15H). ^{13}C NMR (150 MHz, $CDCl_3$) δ = 154.95, 154.91, 154.15, 154.09, 141.90, 140.63, 140.58, 140.52, 139.47, 139.27, 138.38, 138.31, 137.30, 137.09, 126.27, 126.18, 125.05, 124.44, 124.36, 123.38, 123.16, 122.96, 122.48, 121.10, 120.69, 120.57, 117.15, 113.64, 113.29, 112.36, 110.11, 109.76, 109.64, 104.21, 103.90, 103.88, 103.83, 103.56, 103.50, 103.40, 103.26, 72.00, 71.91, 71.87, 70.74, 70.65, 70.61, 69.82, 69.70, 69.65, 67.59, 67.37, 67.29, 59.09, 59.03, 58.99. MS(MALDI-TOF) [m/z]: calcd for $C_{92}H_{90}N_6O_5$, 1518.650; found, 1519.251. Anal. Calcd for $C_{92}H_{90}N_6O_5$: C, 72.71; H, 5.97; N, 5.53. Found: C, 72.70; H, 5.98; N, 5.52.

The synthesis of (2R,4R)-2,3,4,5,6-pentakis(4-(nonyloxy)-9H-carbazol-9-yl)benzonitrile (5CzBN-Non)

The synthetic route of 5CzBN-Non was similar to that of 5CzBN-Eth, when the Cz-2C was replaced with Cz-9C. Similarly, the precipitate was purified by column chromatography on silica gel with the petroleum ether and dichloromethane (v:v=2:1, R_f=0.28), and the bright green-yellow product was obtained with a considerable yield (75%). ^{1}H NMR (600 MHz, $CDCl_3$) δ = 8.02-7.99 (t, J=9.0 Hz, 2H), 7.60-7.55 (m, 3H), 7.24-7.20 (m, 1H), 7.17-7.14 (m, 2H), 7.11-7.04 (m, 6H), 6.99-6.95 (m, 2H), 6.94-6.89 (m, 1H), 6.88-6.70 (m, 7H), 6.66-6.46 (m, 8H), 6.30-6.08 (m, 3H), 4.05-4.01 (m,

4H), 3.89-3.74 (m, 6H), 1.92-1.79 (m, 4H), 1.75-1.64 (m, 6H), 1.57-1.44 (m, 5H), 1.44- 1.18 (m, 55H), 0.88 (m, 15H). ^{13}C NMR (150 MHz, $CDCl_3$) δ = 155.42, 155.38, 154.63, 142.13, 140.71, 140.68, 140.65, 140.57, 140.52, 139.57, 139.38, 138.41, 138.34, 137.38, 137.21, 126.20, 125.03, 124.24, 123.59, 123.31, 123.21, 123.04, 122.97, 122.23, 120.98, 120.93, 120.46, 120.39, 120.34, 117.16, 113.45, 113.15, 112.44, 110.14, 109.79, 109.63, 103.80, 103.47, 103.09, 102.83, 102.68, 67.98, 67.78, 67.73, 31.90, 31.87, 29.54, 29.51, 29.47, 29.43, 29.41, 29.39, 29.36, 29.34, 29.30, 29.28, 29.26, 29.25, 29.23, 29.21, 29.17, 26.16, 26.05, 26.01, 22.69, 22.66, 14.12, 14.10. MS(MALDI-TOF) [m/z]: calcd for $C_{112}H_{130}N_6O_5$, 1639.010; found, 1639.886. Anal. Calcd for $C_{112}H_{130}N_6O_5$: C, 82.01; H, 7.99; N, 5.12. Found: C, 82.00; H, 7.98; N, 5.14.

The synthesis of (2R,4R)-2,3,4,5,6-pentakis(4-(dodecyloxy)-9H-carbazol-9-yl)benzonitrile (5CzBN-Dod)

The synthetic route of 5CzBN-Dod was similar to that of 5CzBN-Eth, when the Cz-2C was replaced with Cz-12C. Similarly, the precipitate was purified by column chromatography on silica gel with the petroleum ether and dichloromethane (v:v=2:1, R_f=0.3), and the bright green-yellow product was obtained with a considerable yield (72%). ^{1}H NMR (600 MHz, $CDCl_3$) δ = 8.01-7.98 (t, J=8.6 Hz, 2H), 7.59-7.54 (m, 3H), 7.24-7.19 (m, 1H), 7.16-7.13 (dd, J=10.3, 5.7 Hz, 2H), 7.09-7.03 (m, 6H), 7.00-6.94 (m, 2H), 6.93-6.88 (m, 1H), 6.86-6.82 (m, 1H), 6.82-6.67 (m, 6H), 6.63-6.45 (m, 8H), 6.20-6.14 (m, 3H), 4.05-4.04 (d, J=5.8 Hz, 4H), 3.88-3.72 (m, 6H), 1.92-1.80 (m, 4H), 1.76-1.63 (m, 6H), 1.56-1.43 (m, 5H), 1.39-1.24 (m, 85H), 0.94-0.81 (m, 15H). ^{13}C NMR (150 MHz, $CDCl_3$) δ = 155.43, 155.37, 154.64, 154.60, 154.54, 142.14, 140.71, 140.65, 140.63, 140.58, 140.52, 139.60, 139.55, 139.41, 138.40, 138.35, 137.39, 137.21, 126.20, 125.01, 124.25, 123.59, 123.23, 123.04, 122.97, 122.23, 121.00, 120.47, 120.41, 117.17, 113.49, 113.15, 112.44, 110.15, 109.79, 109.57, 103.83, 103.49, 103.07, 102.83, 102.68, 68.00, 67.98, 67.78, 31.93, 31.91, 29.70, 29.67, 29.64, 29.61, 29.54, 29.45, 29.43, 29.40, 29.37, 29.36, 29.22, 29.18, 26.17, 26.07, 26.03, 22.70, 22.68, 14.13. MS(MALDI-TOF) [m/z]: calcd for $C_{127}H_{160}N_6O_5$, 1850.710; found, 1851.347. Anal. Calcd for $C_{127}H_{160}N_6O_5$: C, 82.42; H, 8.71; N, 4.54. Found: C, 82.40; H, 8.68; N, 4.58.

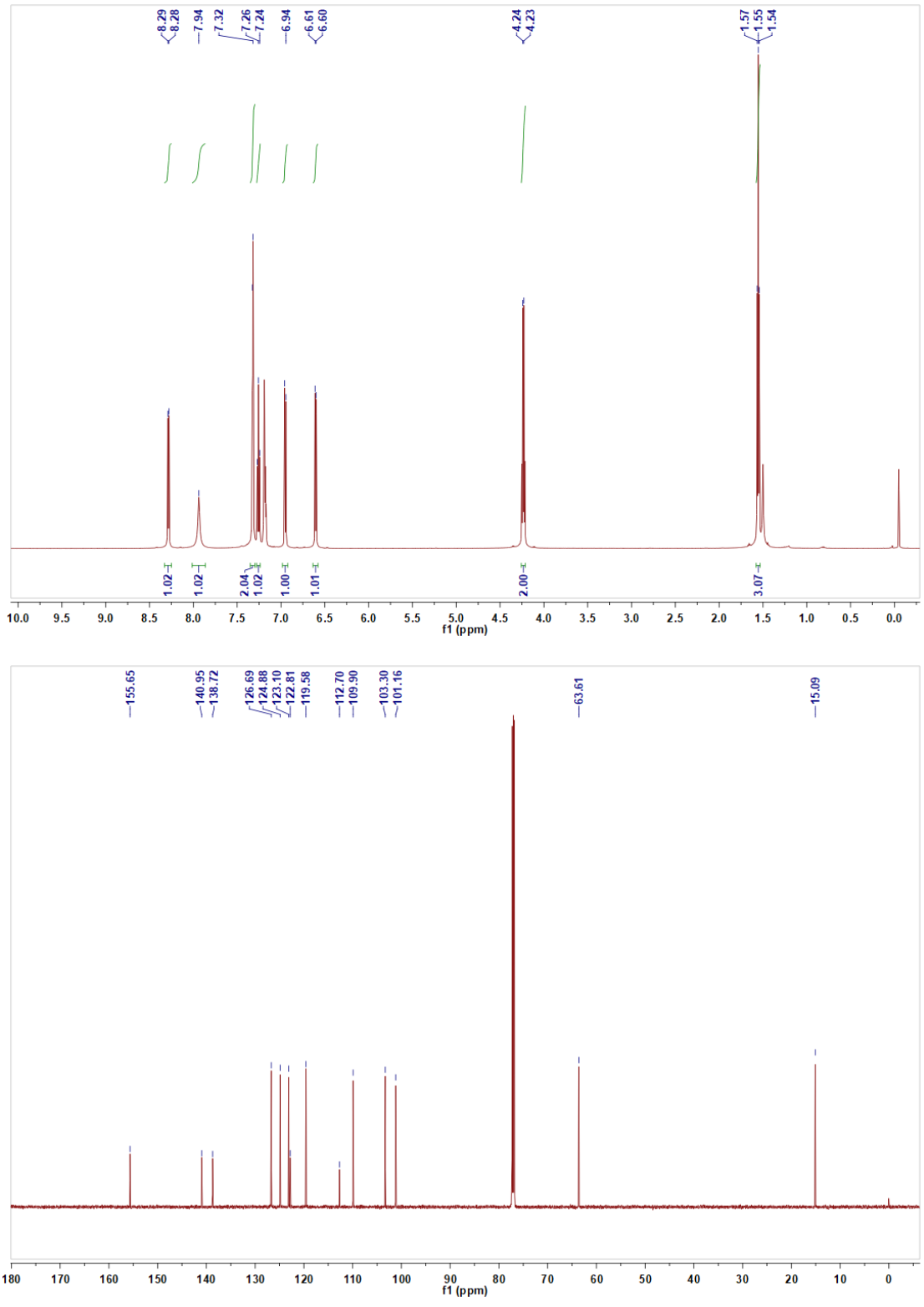

Figure S1. ^{1}H NMR and ^{13}C NMR spectrum of Cz-2C.

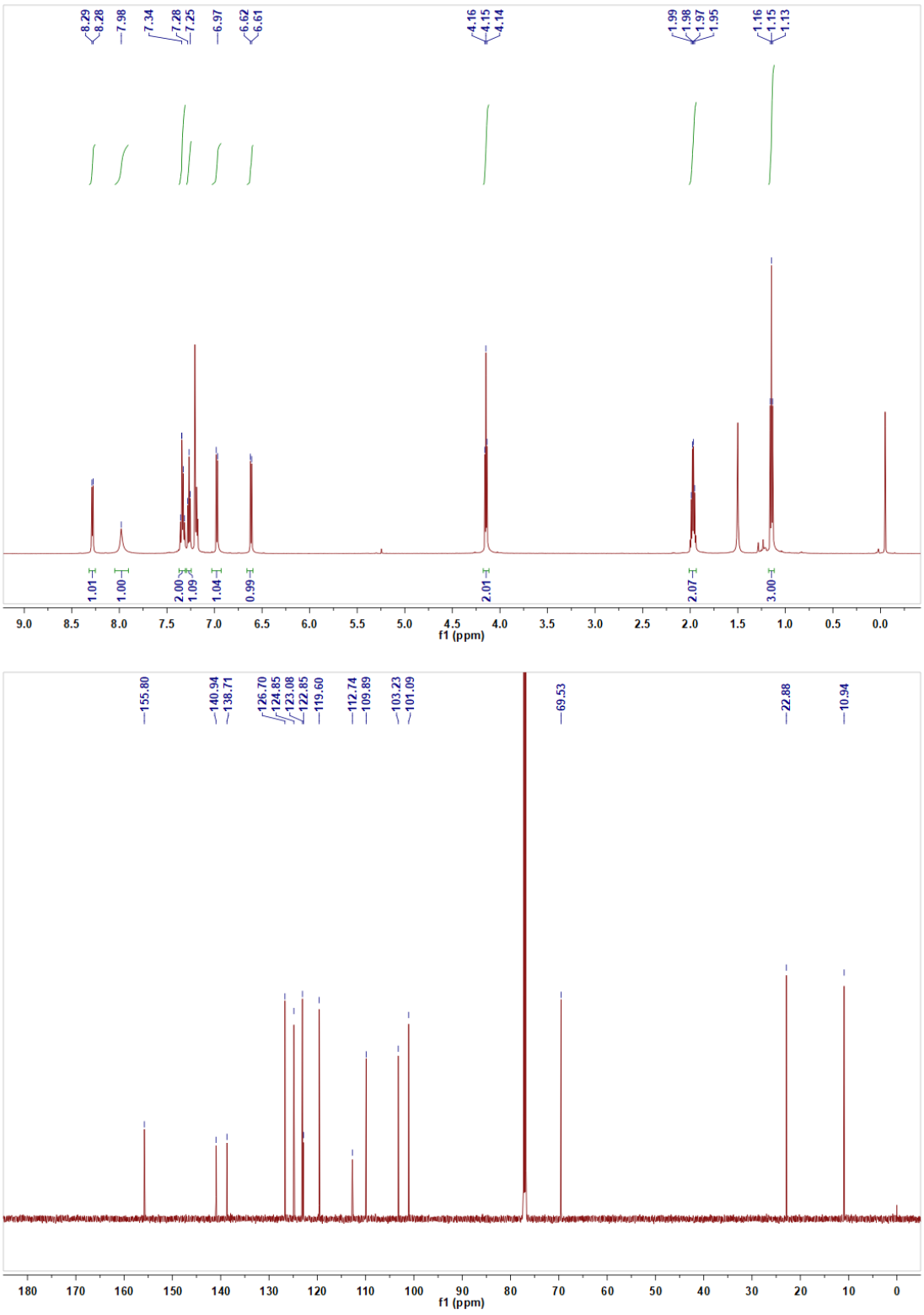

Figure S2. ^{1}H NMR and ^{13}C NMR spectrum of Cz-3C.

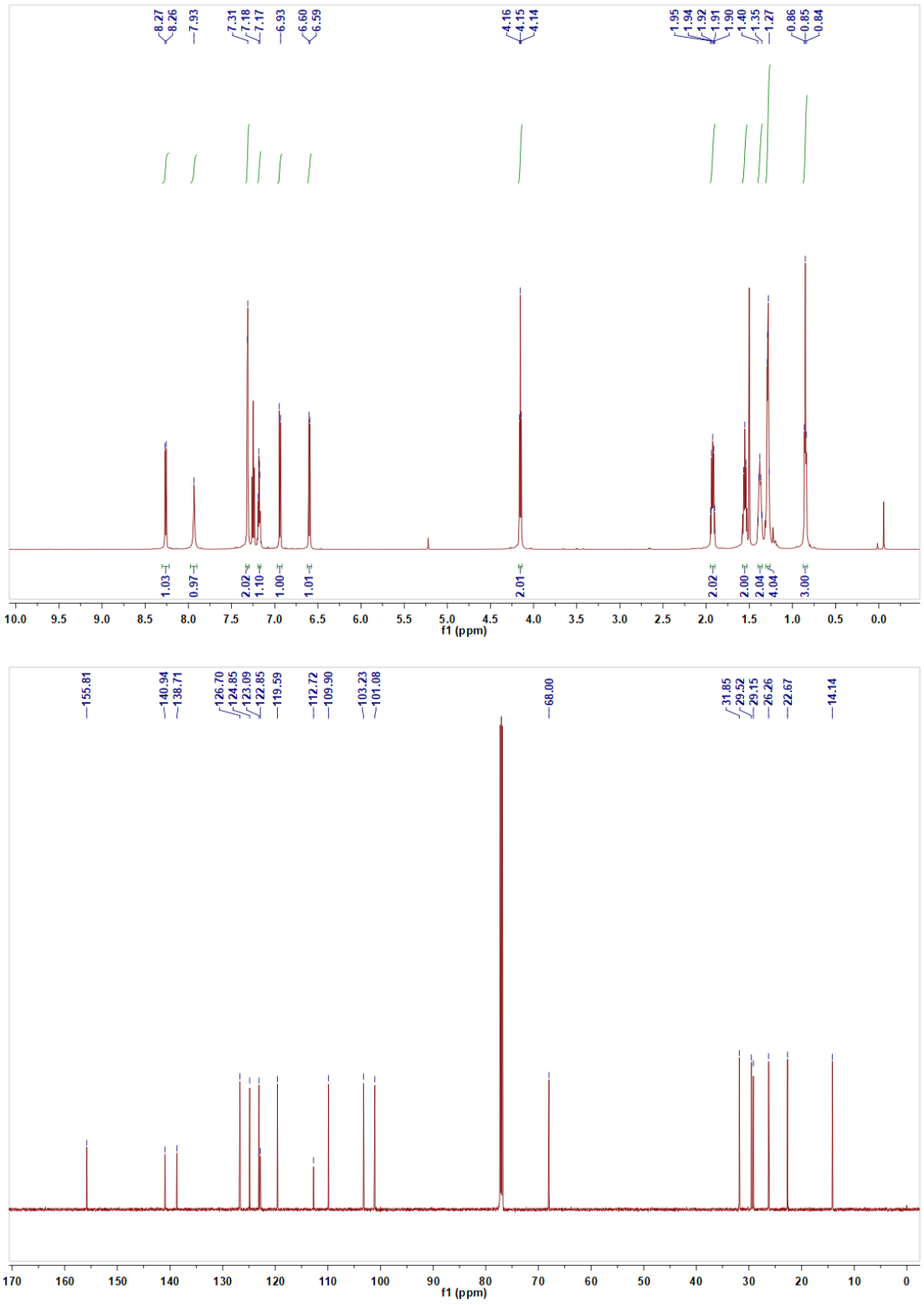

Figure S3. ^{1}H NMR and ^{13}C NMR spectrum of Cz-7C.

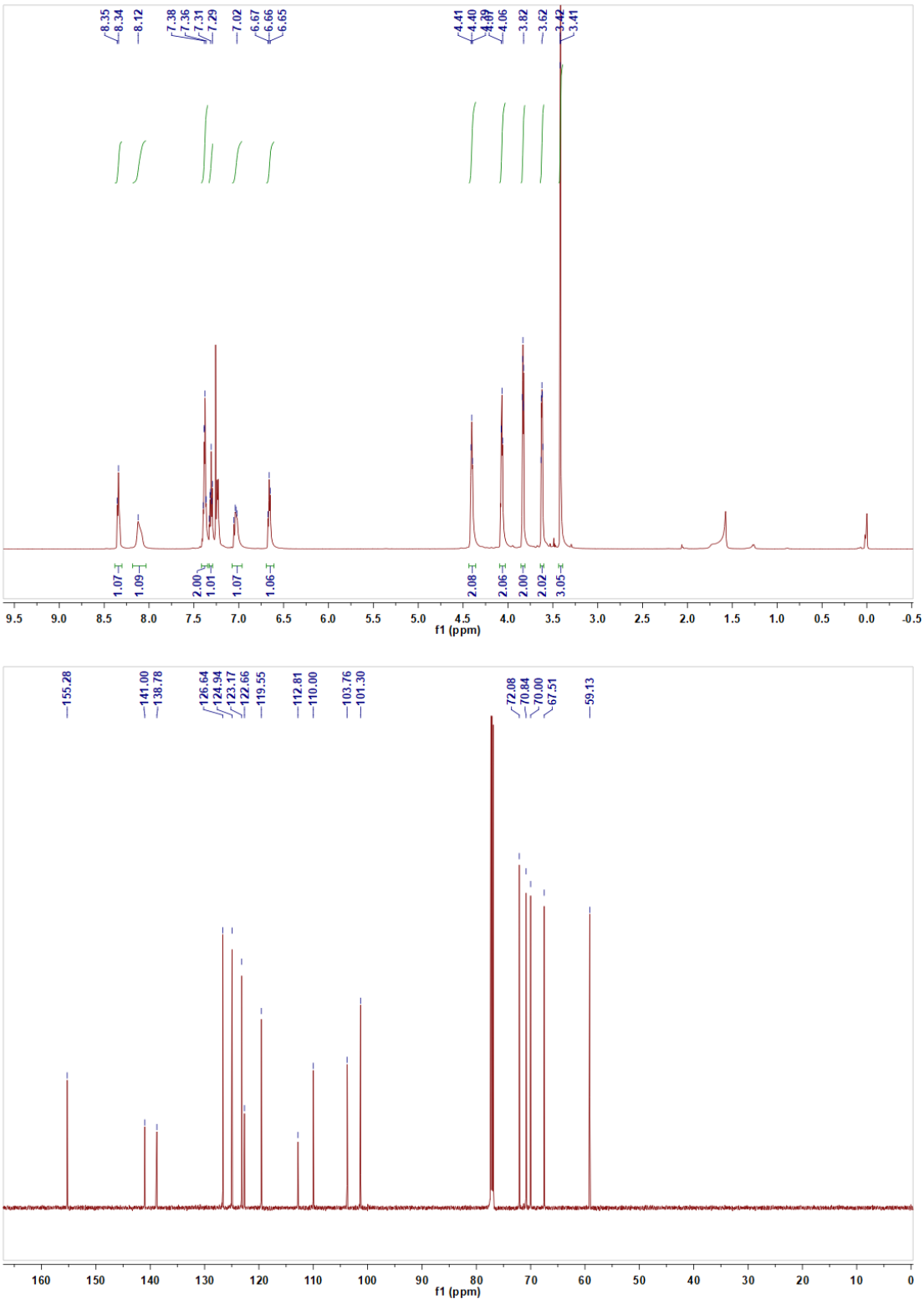

Figure S4. ^{1}H NMR and ^{13}C NMR spectrum of Cz-7O.

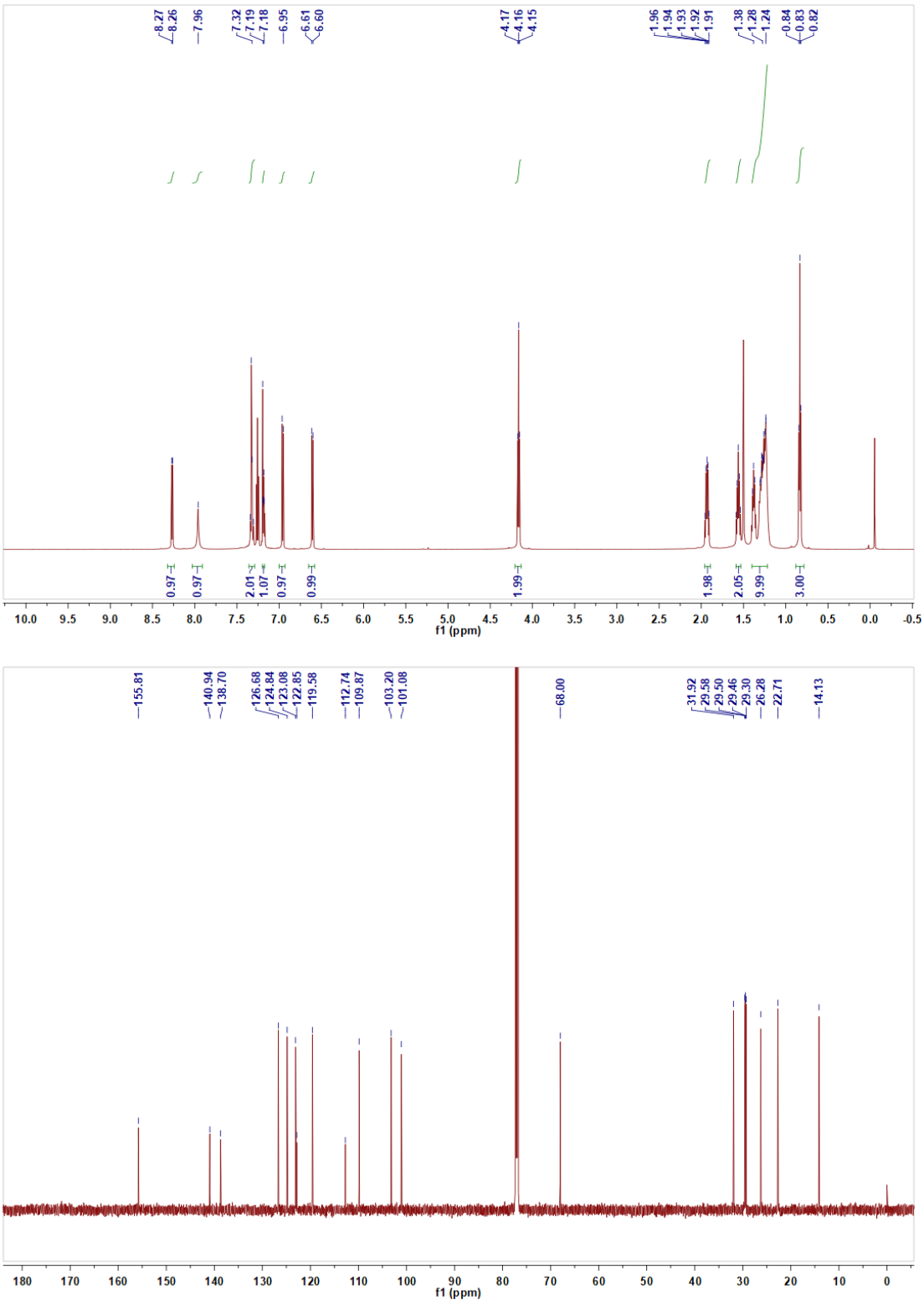

Figure S5. ^{1}H NMR and ^{13}C NMR spectrum of Cz-9C.

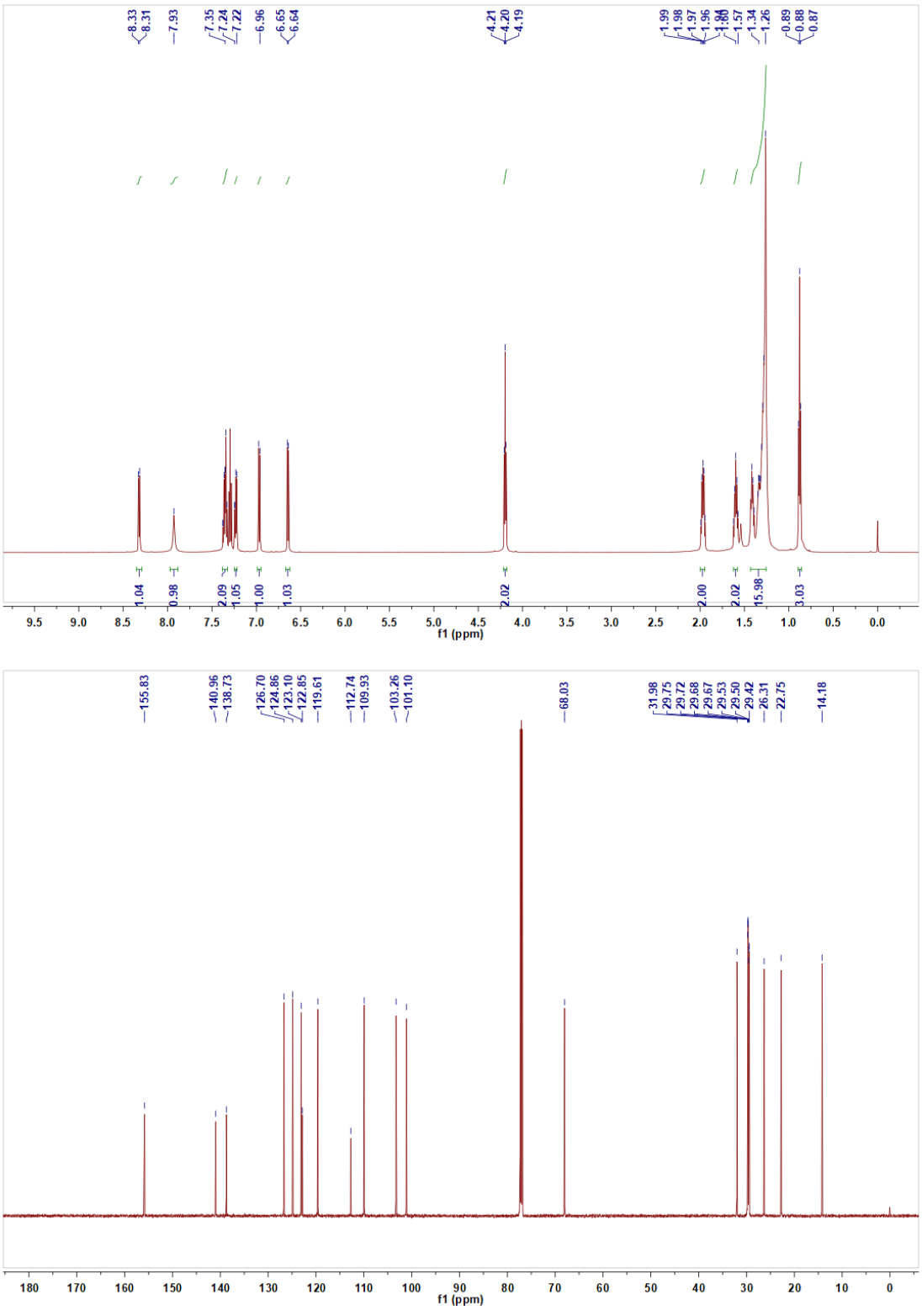

Figure S6. ^{1}H NMR and ^{13}C NMR spectrum of Cz-12C.

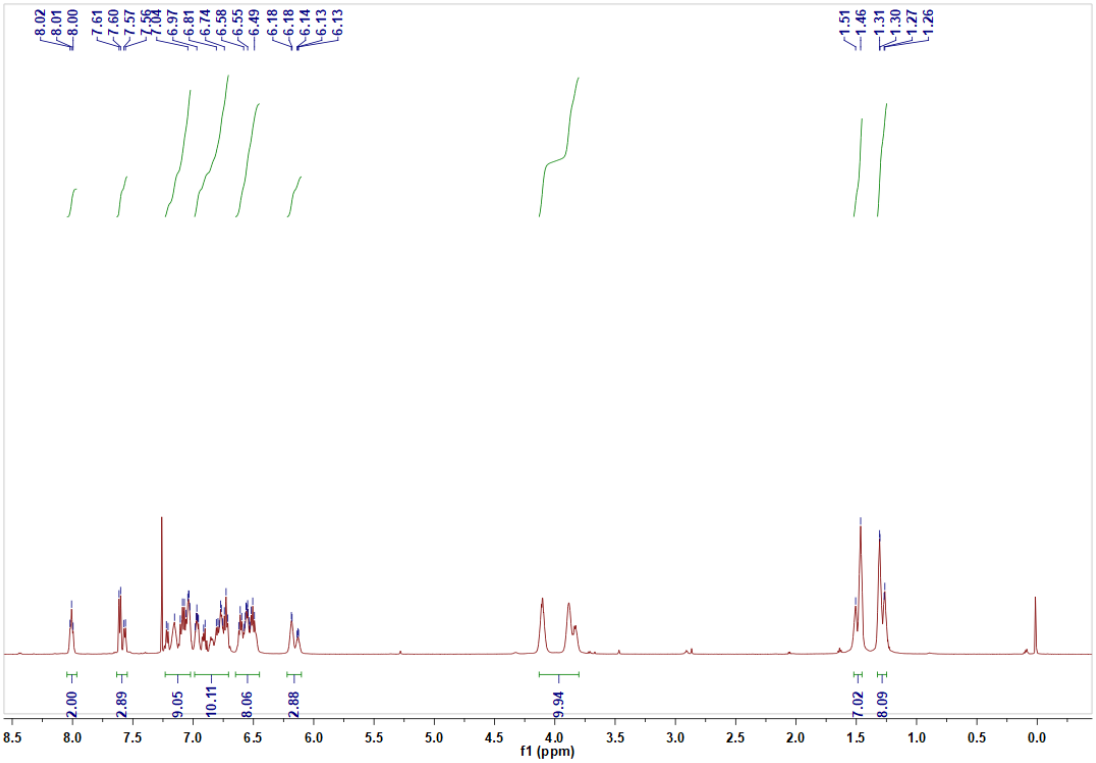
8.02
8.01
8.00
7.61
7.60
7.57
7.56
7.04
6.97
6.81
6.74
6.58
6.55
6.49
6.18
6.18
6.14
6.13
6.13
1.51
1.46
1.31
1.30
1.27
1.26
2.00
2.89
9.05
10.11
8.06
2.88
9.94
7.02
8.09
f1 (ppm)

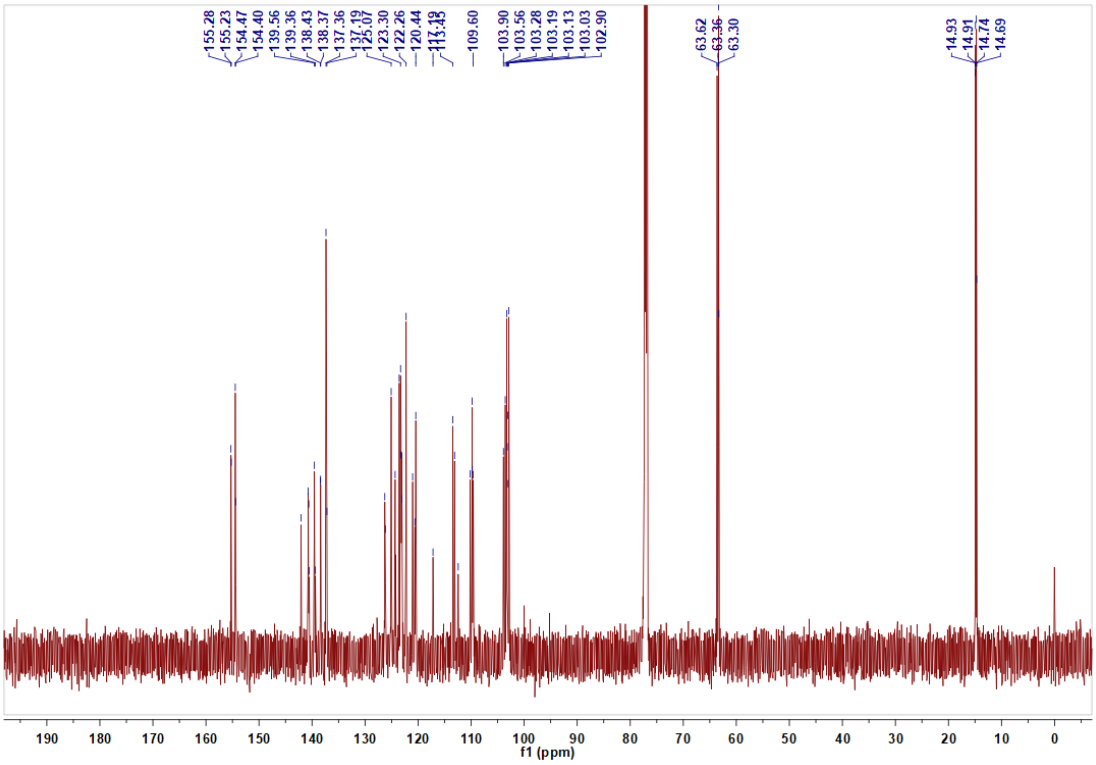
155.28
155.23
154.47
154.40
139.56
139.36
138.43
138.37
137.36
123.30
122.26
120.44
109.60
103.90
103.56
103.28
103.19
103.13
103.03
102.90
63.62
63.36
63.30
14.93
14.91
14.74
14.69
f1 (ppm)

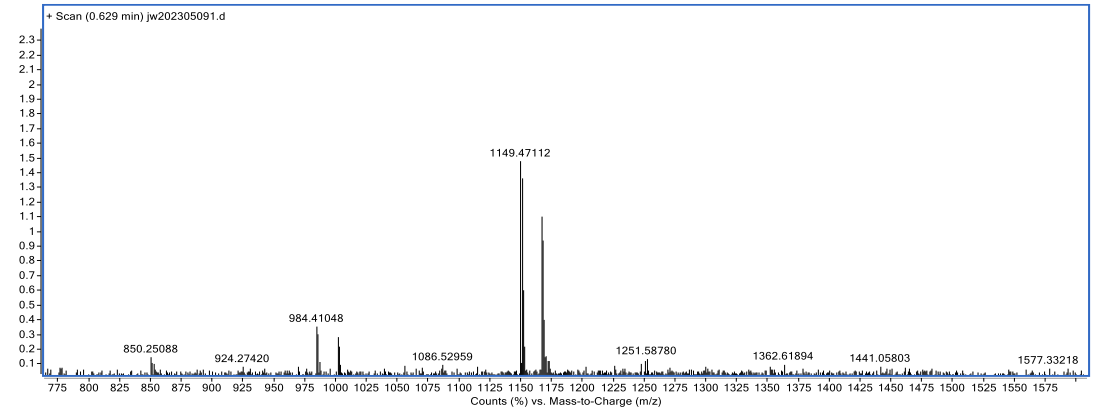

Figure S7. ^{1}H NMR, ^{13}C NMR and high-resolution mass spectra of 5CzBN-Eth.

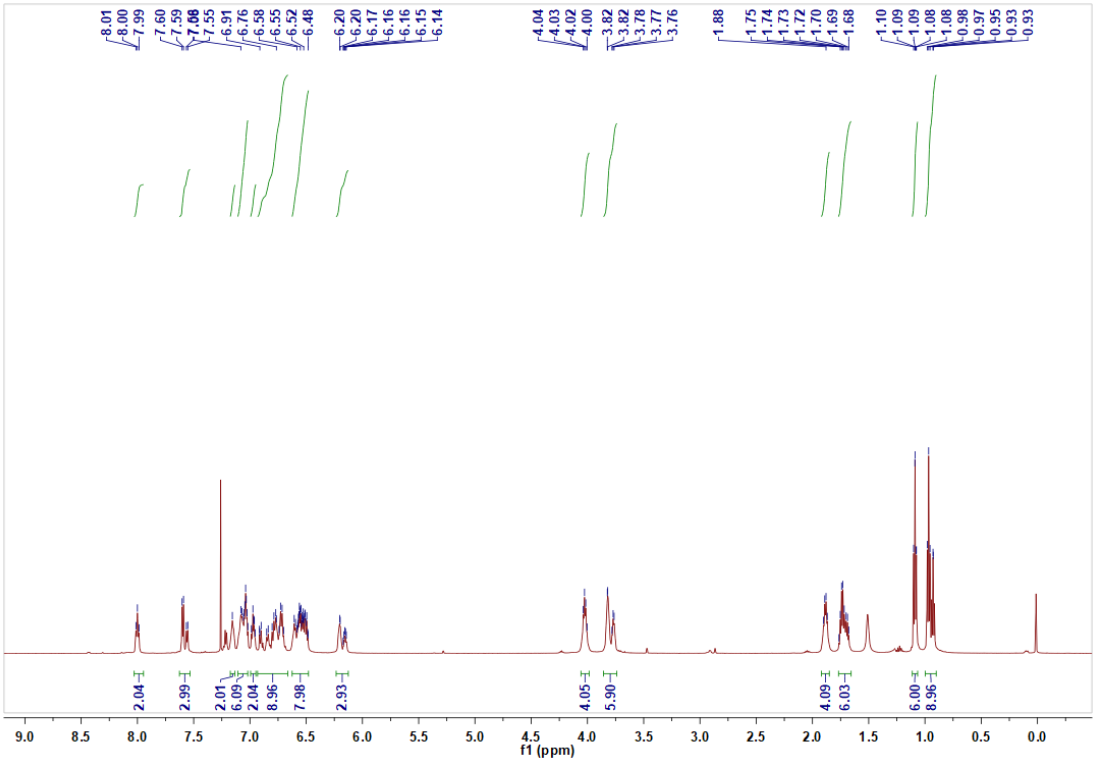

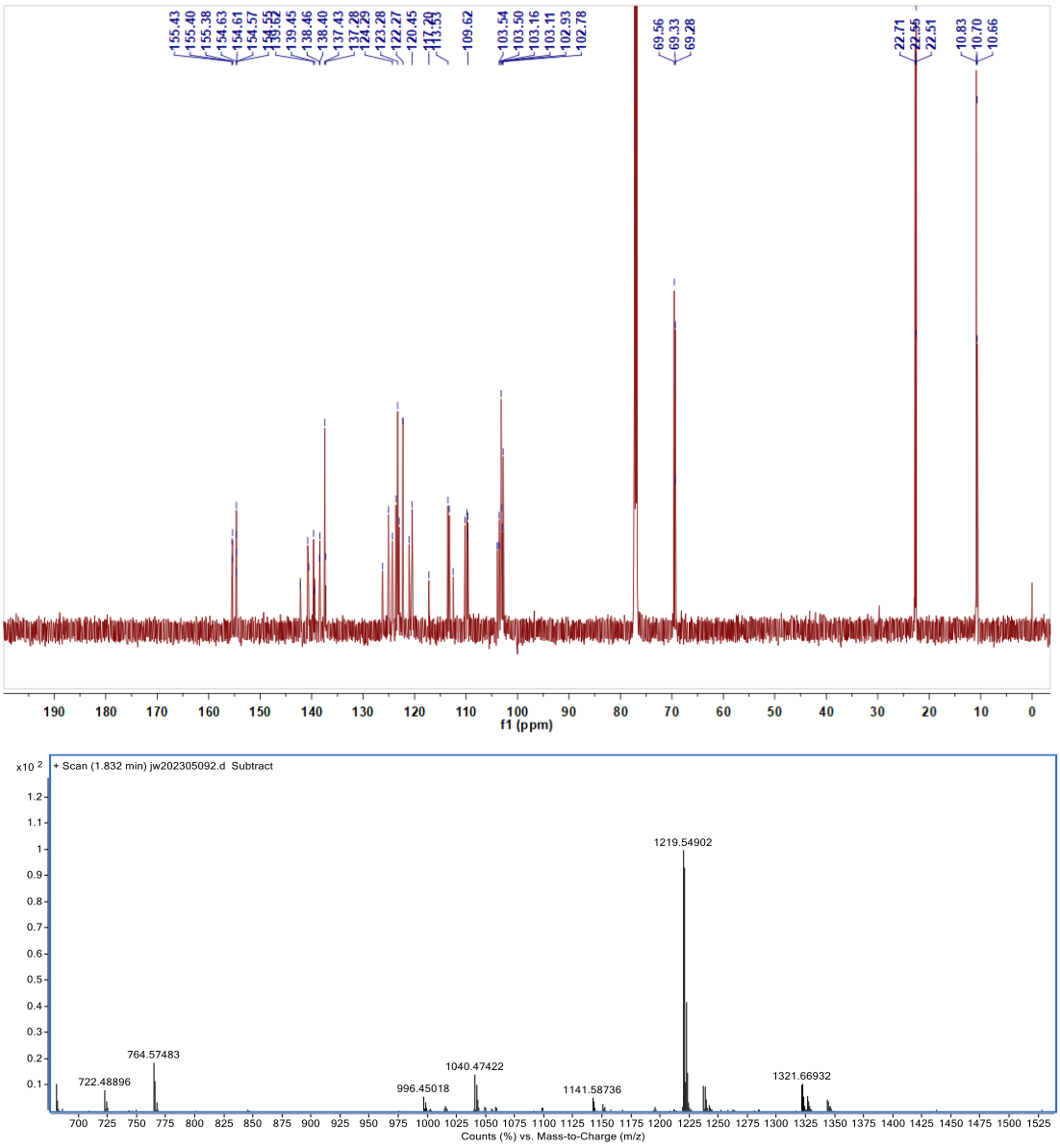

Figure S8. ^{1}H NMR, ^{13}C NMR and high-resolution mass spectra of 5CzBN-Pro.

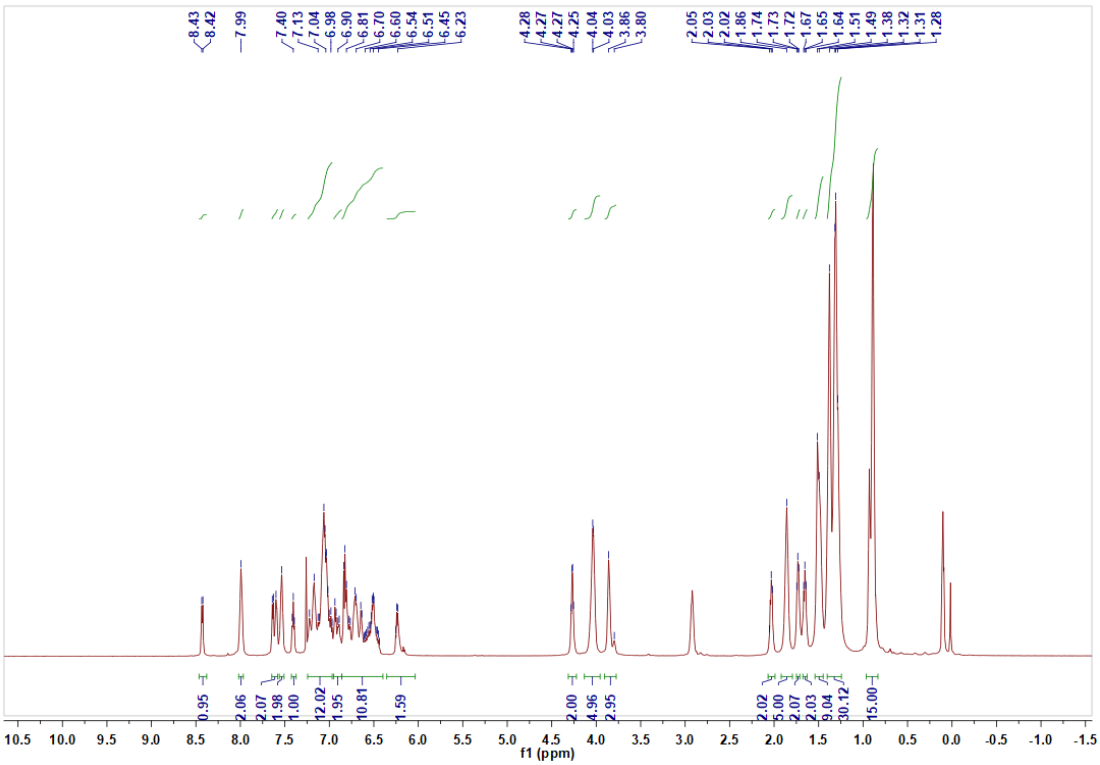
8.43
8.42
7.99
7.40
7.13
7.04
6.98
6.90
6.81
6.70
6.60
6.54
6.51
6.45
6.23
4.28
4.27
4.27
4.25
4.04
4.03
3.86
3.80
2.05
2.03
2.02
1.86
1.74
1.73
1.72
1.67
1.65
1.64
1.51
1.49
1.38
1.32
1.31
1.28
0.95
2.06
2.07
1.98
1.00
12.02
1.95
10.81
1.59
2.00
4.96
2.95
2.02
5.00
2.07
2.03
9.04
30.12
15.00
f1 (ppm)

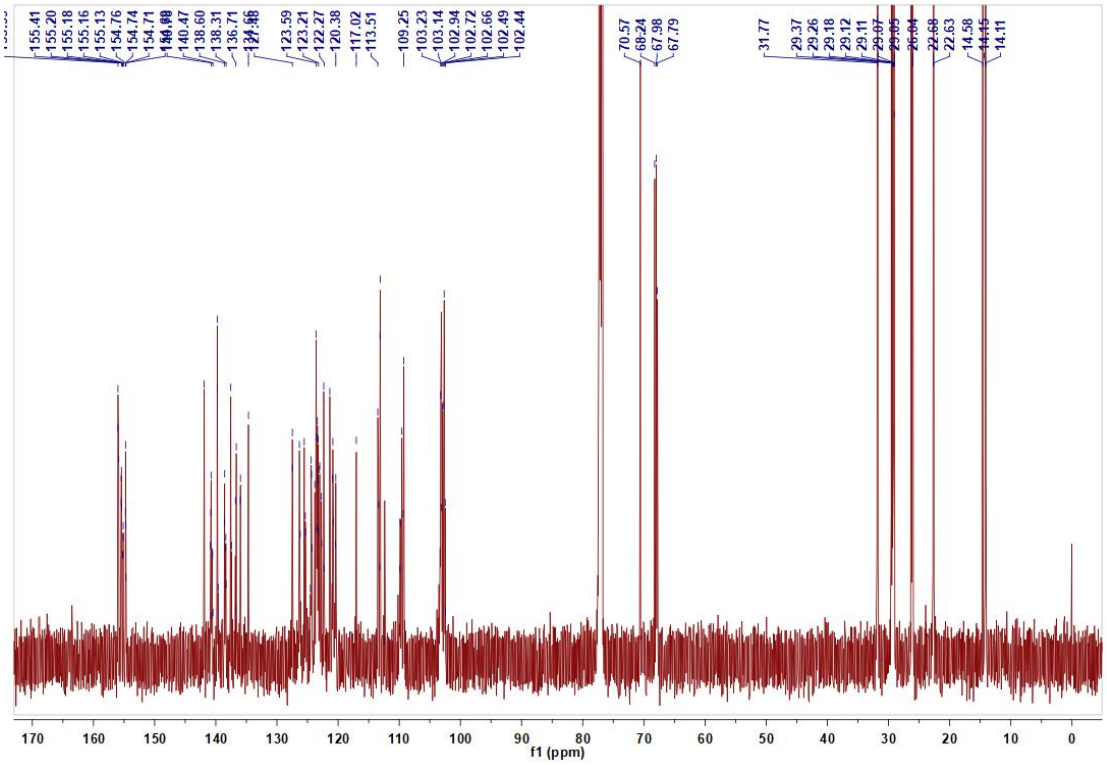
155.41
155.20
155.18
155.16
155.13
154.76
154.74
154.71
140.47
138.60
138.31
136.71
123.59
123.21
122.27
120.38
117.02
113.51
109.25
103.23
103.14
102.94
102.72
102.66
102.49
102.44
70.57
68.24
67.98
67.79
31.77
29.37
29.26
29.18
29.12
29.11
29.07
29.05
26.04
22.68
22.63
14.58
14.15
14.11
f1 (ppm)

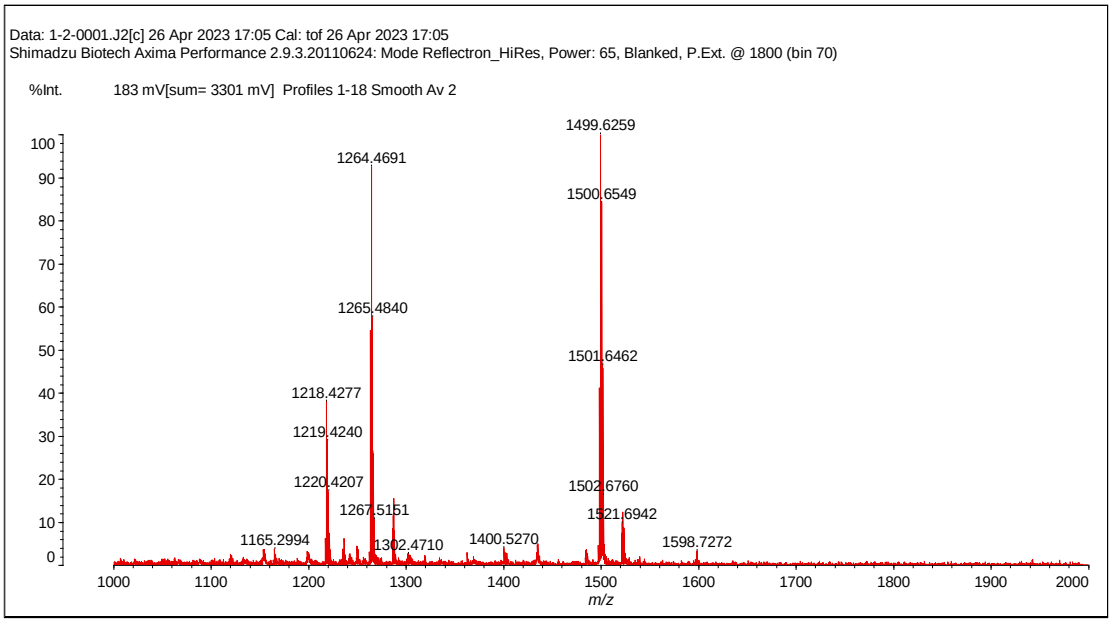

Figure S9. ^{1}H NMR, ^{13}C NMR and MALDI-TOF mass spectra of 5CzBN-Hep.

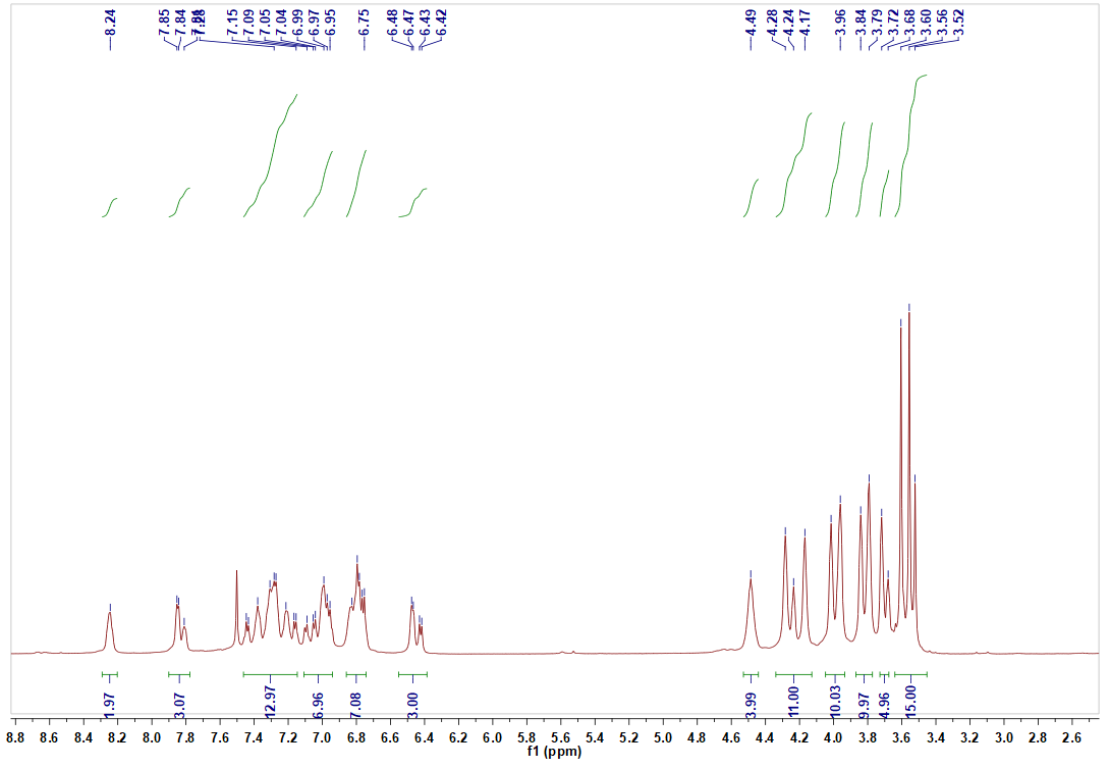

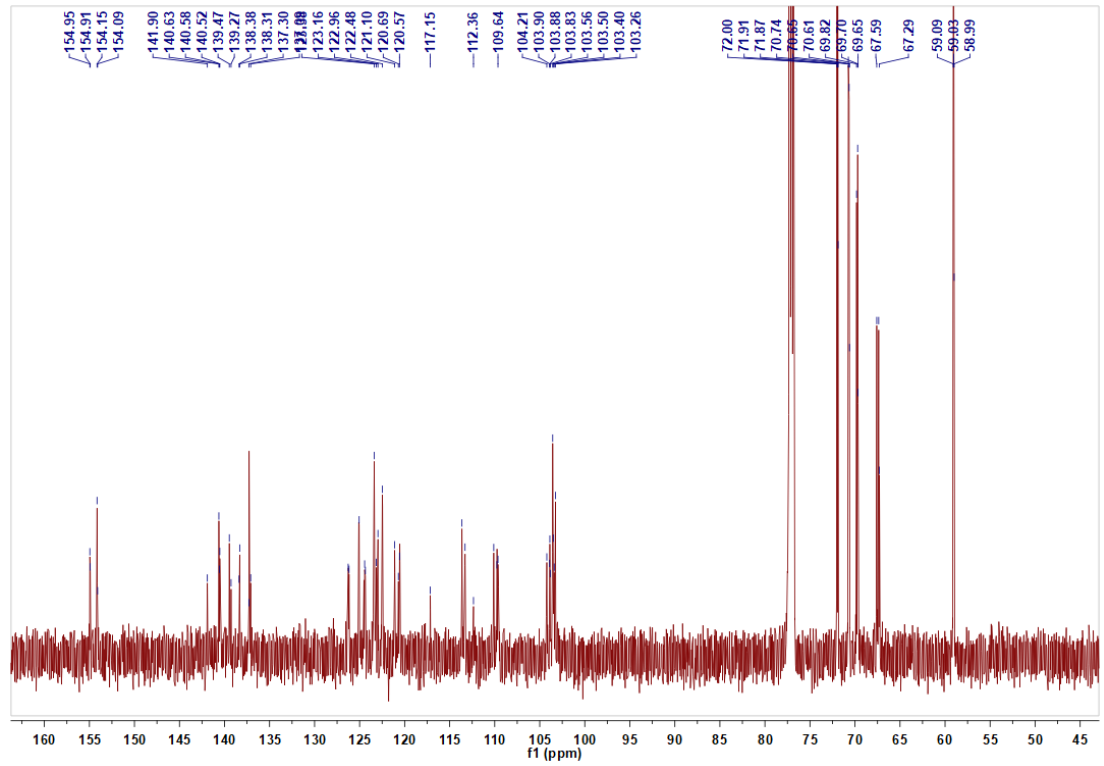

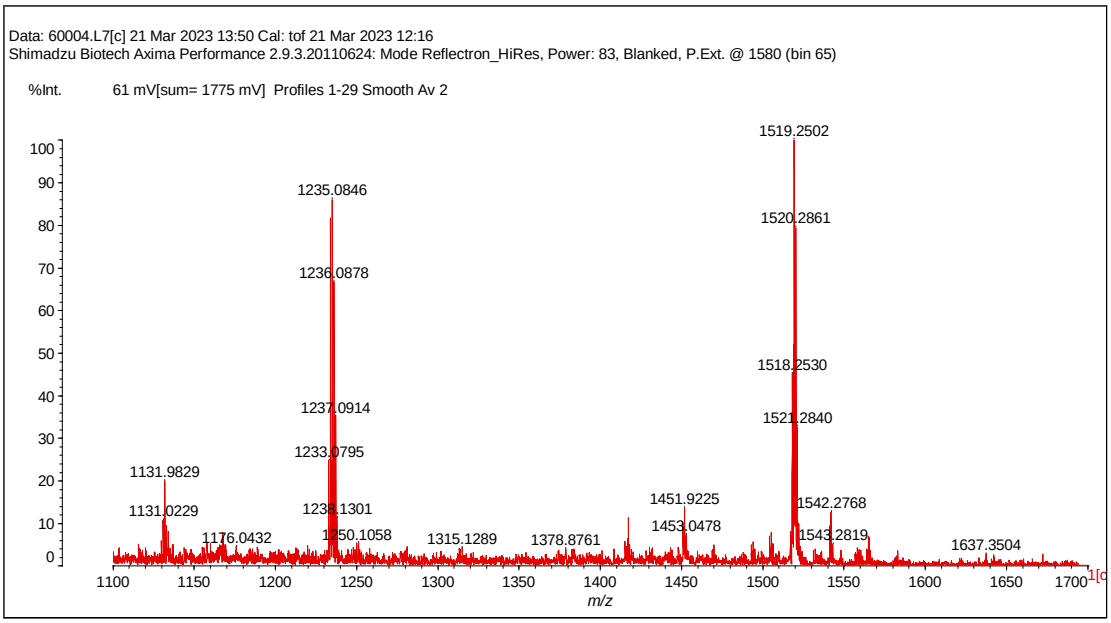

Figure S10. ^{1}H NMR, ^{13}C NMR and MALDI-TOF mass spectra of 5CzBN-OEG.

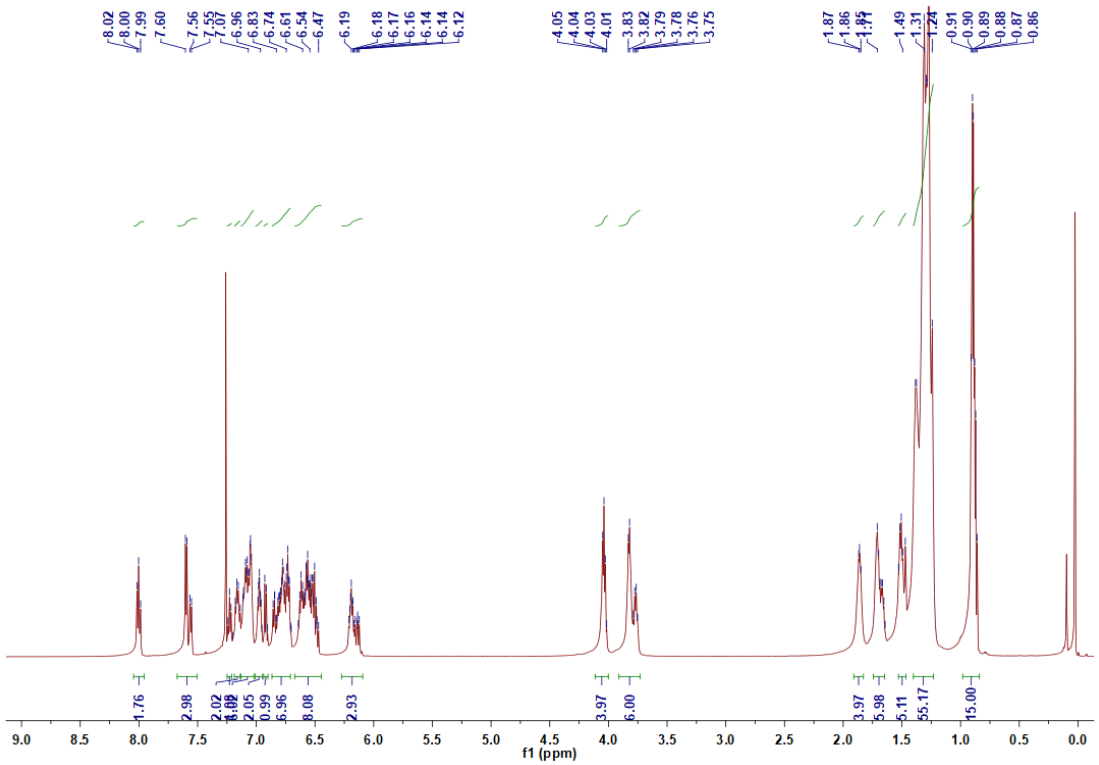
8.02
8.00
7.99
7.60
7.56
7.55
7.07
6.96
6.83
6.74
6.61
6.54
6.47
6.19
6.18
6.17
6.16
6.14
6.14
6.12
4.05
4.04
4.03
4.01
3.83
3.82
3.79
3.78
3.76
3.75
1.87
1.86
1.49
1.31
1.24
0.91
0.90
0.89
0.88
0.87
0.86
1.76
2.98
2.02
2.05
0.99
6.96
8.08
2.93
3.97
6.00
3.97
5.98
5.11
55.17
15.00
f1 (ppm)

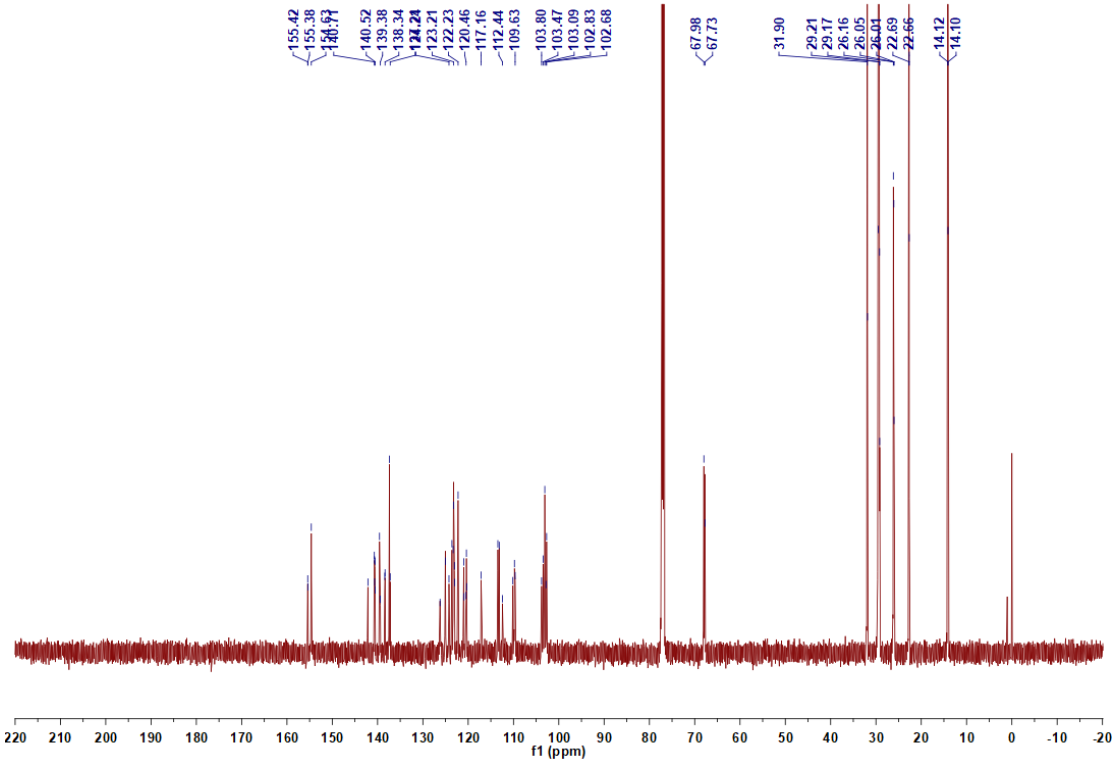
155.42
155.38
140.52
139.38
138.34
123.21
122.23
120.46
117.16
112.44
109.63
103.80
103.47
103.09
102.83
102.68
67.98
67.73
31.90
29.21
29.17
26.16
26.05
22.69
22.66
14.12
14.10
f1 (ppm)

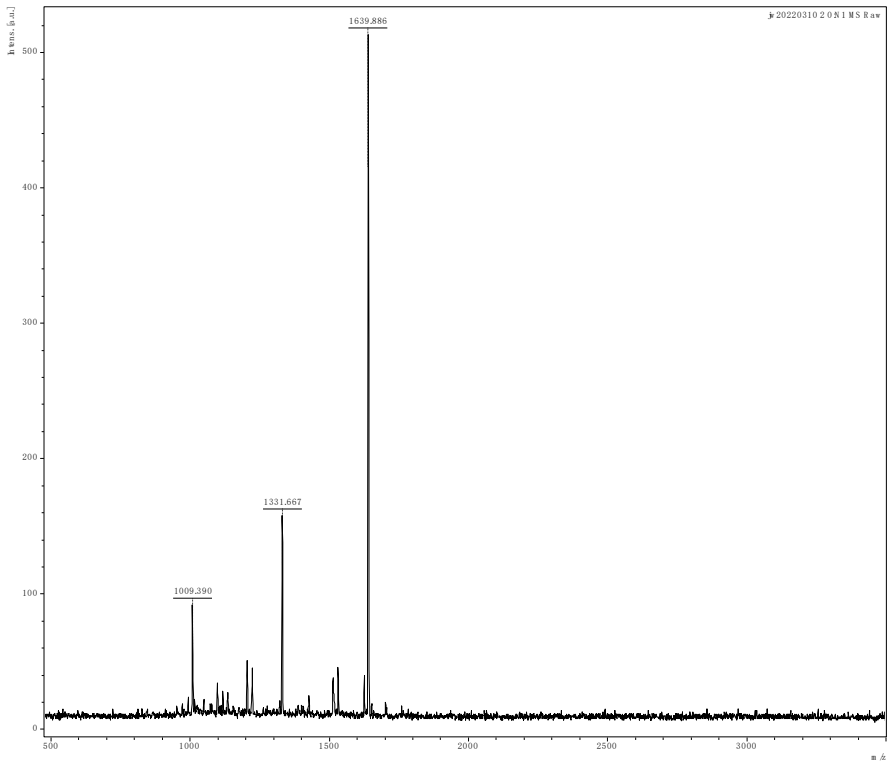

Figure S11. ^{1}H NMR, ^{13}C NMR and MALDI-TOF mass spectra of 5CzBN-Non.

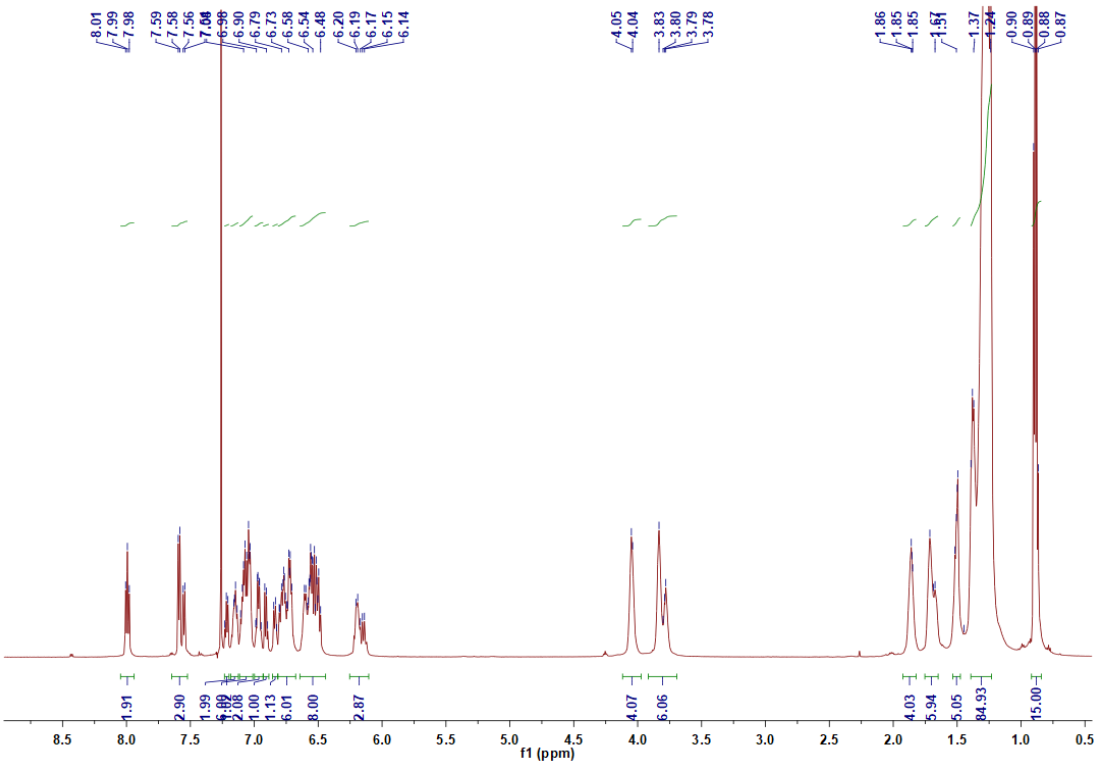

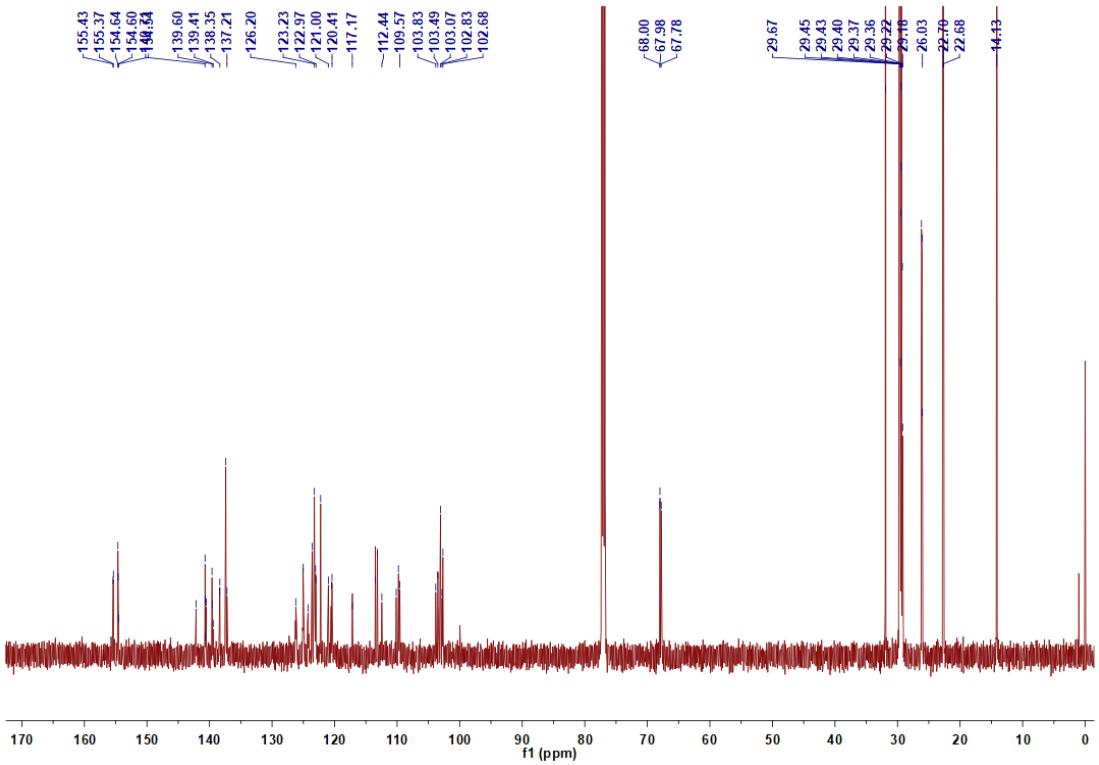

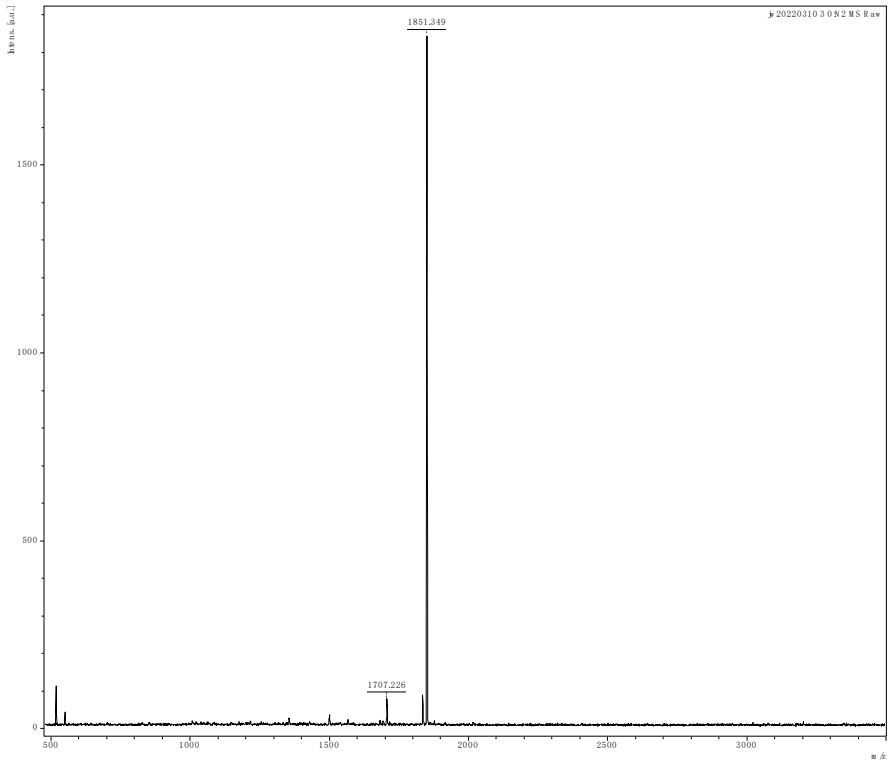

Figure S12. ^{1}H NMR, ^{13}C NMR and MALDI-TOF mass spectra of 5CzBN-Dod.

3. *Supplementary figures and tables*

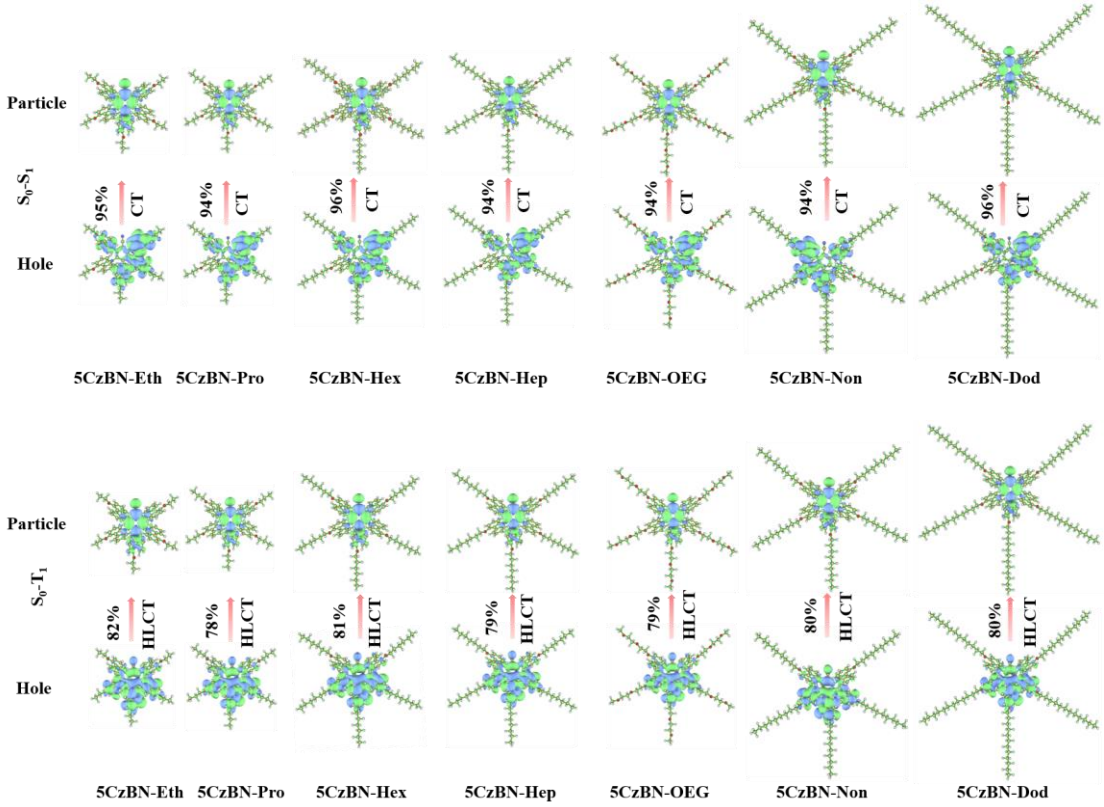

Figure S13. The calculated natural transition orbitals (NTOs) of S_1 and T_1 states for 5CzBN derivatives in B3LYP/6-31G(d) level under gas phase.

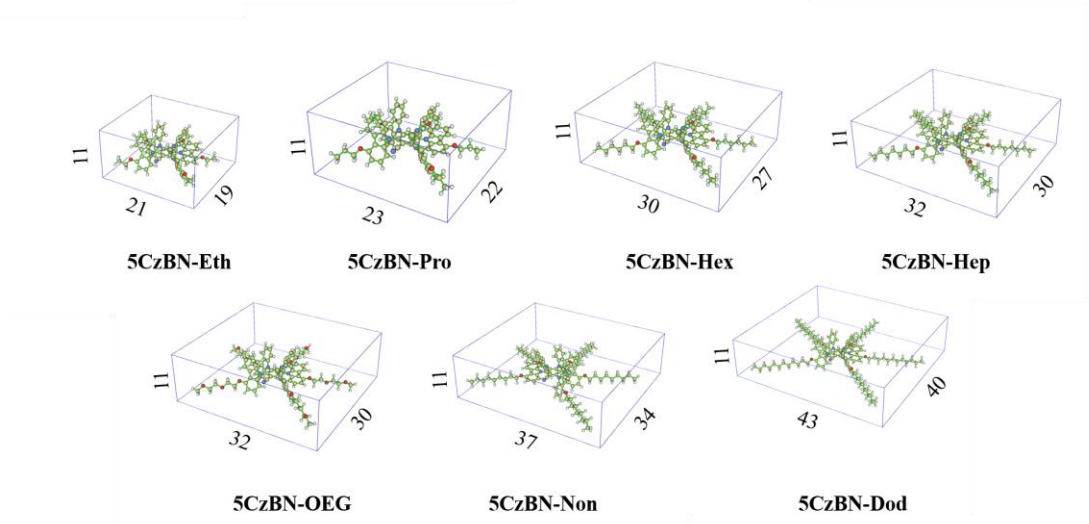

Figure S14. Calculated length, width, and height (Å) of 5CzBN derivatives at B3LYP/6-31g(d) level.

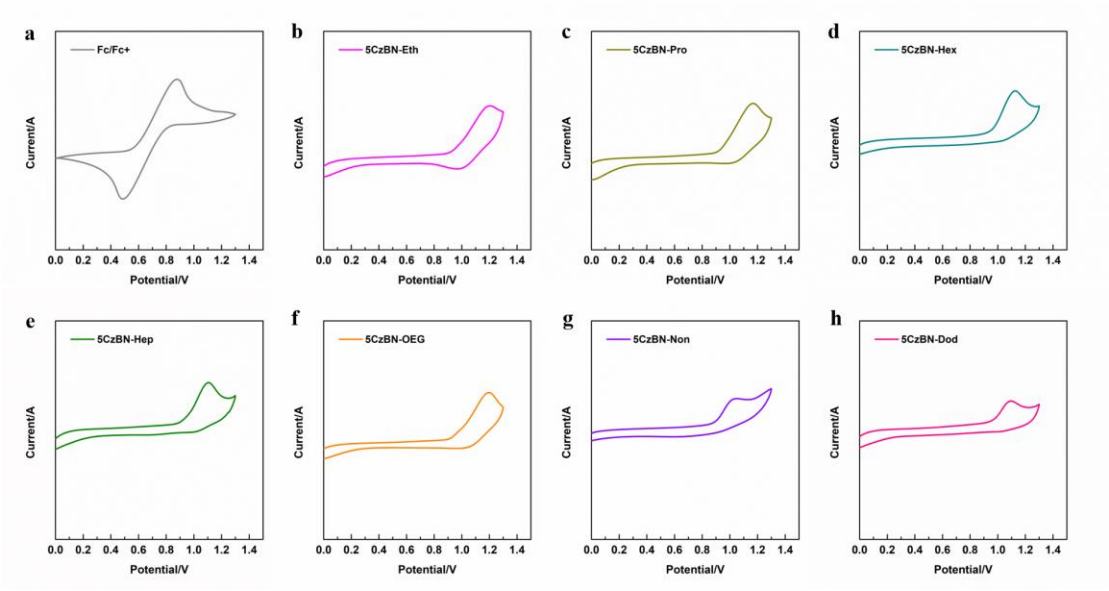

Figure S15. The cyclic voltammogram of 5CzBN derivatives.

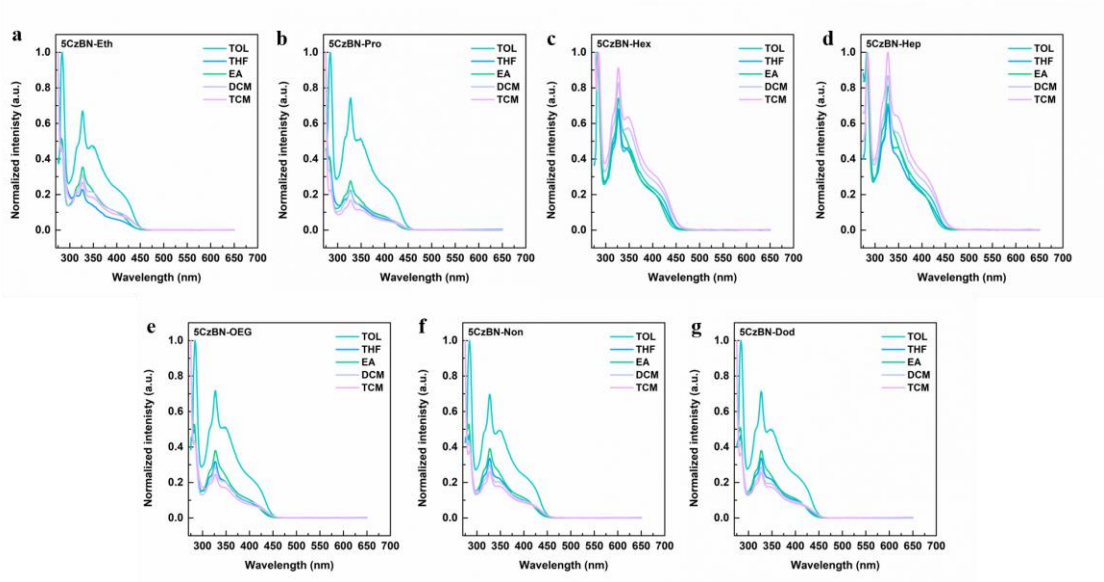

Figure S16. The normalized absorption spectra of 5CzBN derivatives in different solution with a concentration of 10^{-5} M (Tol: toluene, EA: ethyl acetate, THF: tetrahydrofuran, DCM: dichloromethane, TCM: trichloromethane).

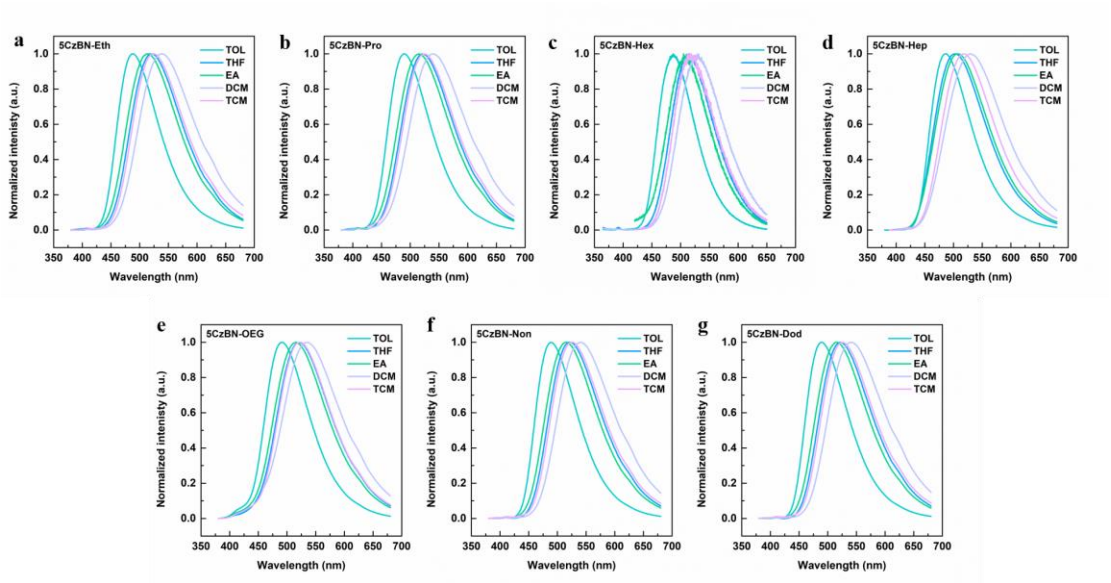

Figure S17. The normalized PL spectra of 5CzBN derivatives in different solution with a concentration of 10^{-5} M (Tol: toluene, EA: ethyl acetate, THF: tetrahydrofuran, DCM: dichloromethane, TCM: trichloromethane).

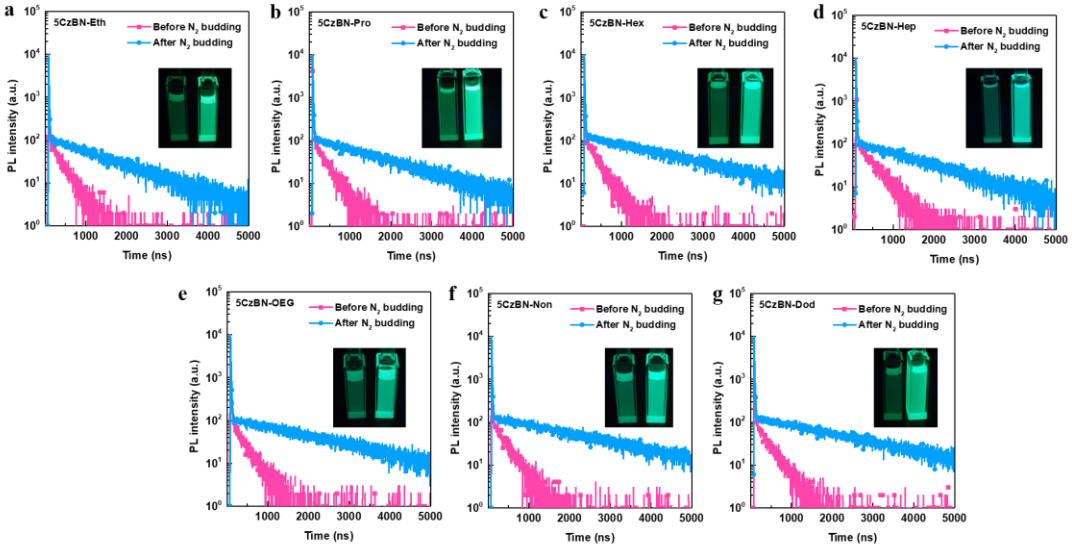

Figure S18. Transient PL decay curves of 5CzBN derivatives in toluene solution before and after N_2 bubbling for 10 min with a laser of 375 nm.

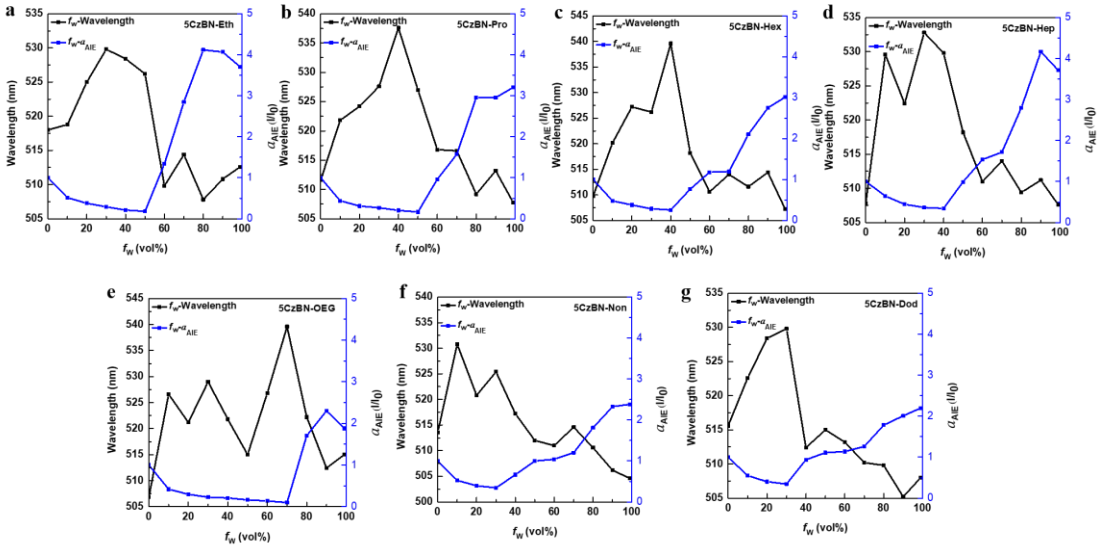

Figure S19. The emission wavelength versus the water volume fraction and the plots of the fluorescence ratio (α_{AIE}=I/I$_0$) versus the water volume fraction of THF/H_2O solution with an excitation wavelength of 375 nm.

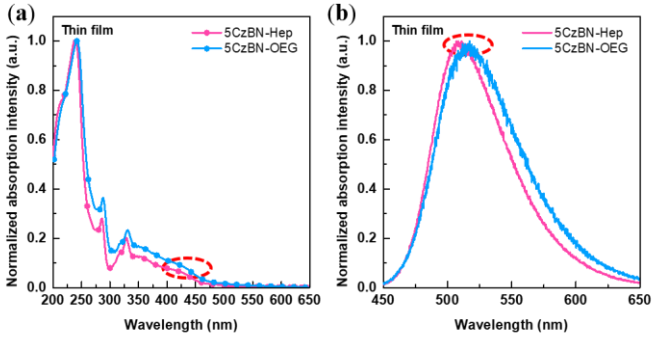

Figure S20. (a) UV-vis absorption of 5CzBN-Hep and 5CzBN-OEG in thin film. (b) PL spectra of 5CzBN-Hep and 5CzBN-OEG in thin film.

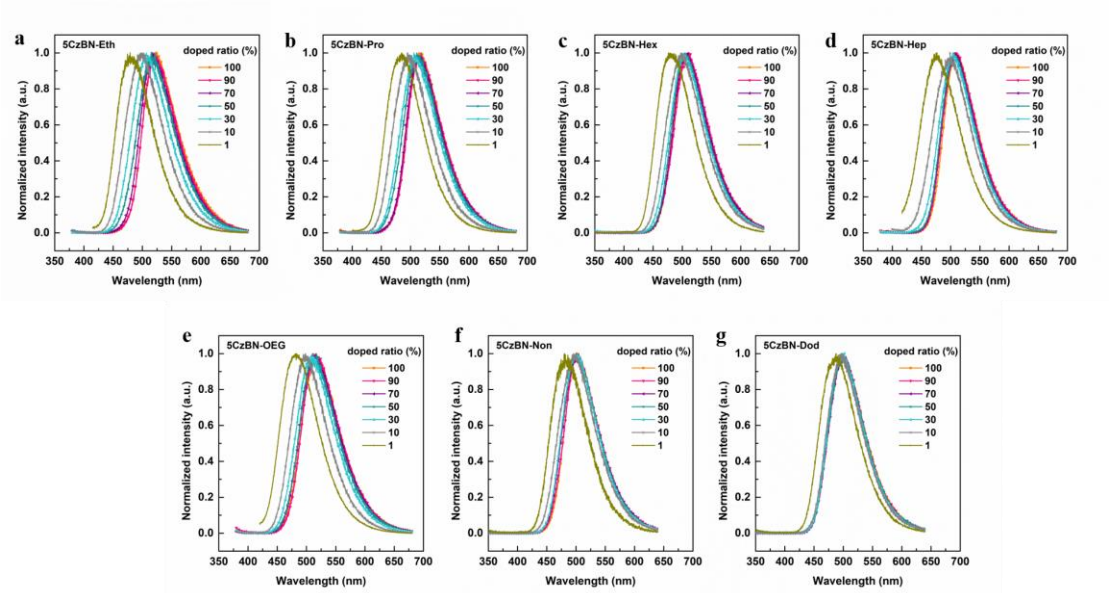

Figure S21. The normalized PL spectra of 5CzBN derivatives doped films in PMMA matrix with various doping concentration at 300 K (Insert: the enlarged figures of doped PL spectra to analyze the intermolecular interaction).

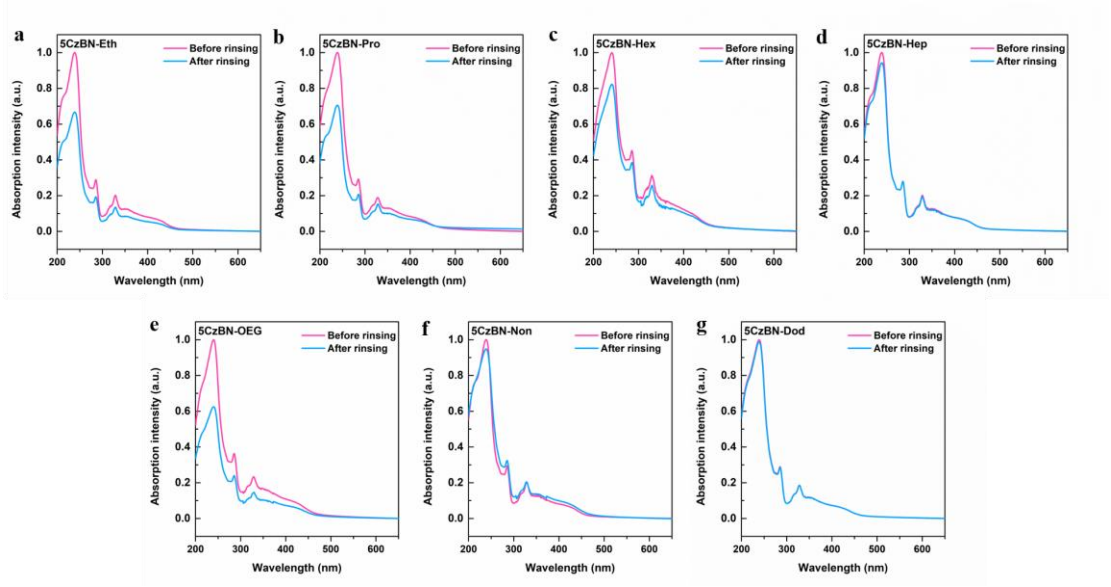

Figure S22. The absorption spectra before and after rinsing with isopropanol of the solution-processed films of 5CzBN derivatives.

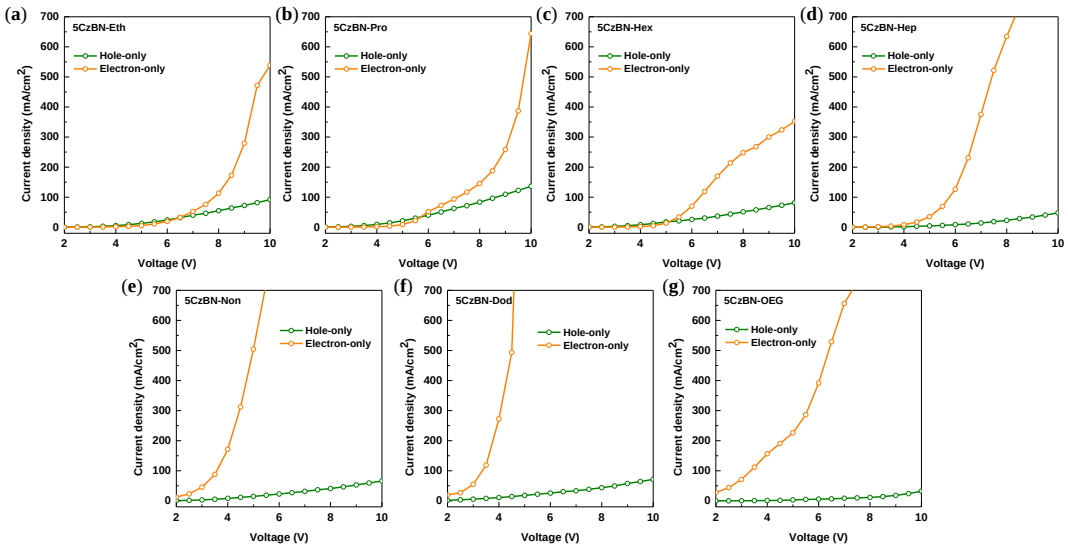

Figure S23. The IV characteristics of electron-only devices with a configuration of ITO|Al (50 nm)|EML (40 nm)|POT2T(30 nm) |Cs_2CO_3(1 nm) |Al (100 nm), and IV characteristics of hole-only devices with configurations of ITO|PEDOT:PSS (40 nm)|EML (40 nm)|MoO_3 (20 nm)|Al (100 nm) based on 5CzBN derivatives.

Table S1. The calculated data of 5CzBN derivatives.

Compound	HOMO (eV)	LUMO (eV)	E_g (eV)	f	μ_0 (Debye)	S_1 (eV)	T_1 (eV)	ΔE_{ST} (eV)
5CzBN-Eth	-5.17	-1.95	3.22	0.0299	5.5526	2.62	2.48	0.14
5CzBN-Pro	-5.16	-1.94	3.22	0.0306	5.4715	2.62	2.48	0.14
5CzBN-Hex	-5.14	-1.93	3.21	0.0305	5.6001	2.61	2.48	0.13
5CzBN-Hep	-5.14	-1.92	3.22	0.0319	5.4723	2.62	2.48	0.14
5CzBN-Non	-5.13	-1.92	3.21	0.0306	5.3836	2.62	2.48	0.14
5CzBN-Dod	-5.13	-1.92	3.21	0.0307	5.5469	2.62	2.48	0.14
5CzBN-OEG	-5.15	-1.93	3.20	0.0292	6.0095	2.63	2.49	0.14

Table S2. The experimental peaks of PL spectra of 5CzBN derivatives doped in PMMA matrix.

Compound	1 wt% λ_{PL} (nm)	10 wt% λ_{PL} (nm)	30 wt% λ_{PL} (nm)	50 wt% λ_{PL} (nm)	70 wt% λ_{PL} (nm)	90 wt% λ_{PL} (nm)	100 wt% λ_{PL} (nm)
5CzBN-Eth	476.0	497.4	506.8	516.0	517.4	519.8	524.0
5CzBN-Pro	474.4	495.4	505.8	510.6	510.8	518.6	520.0
5CzBN-Hex	476.2	497.0	505.6	503.8	503.8	503.8	507.2
5CzBN-Hep	476.4	497.4	506.2	504.6	504.8	507.3	506.8
5CzBN-Non	475.4	495.6	498.8	500.4	500.2	504.8	502.0
5CzBN-Dod	475.8	496.2	501.8	496.6	497.4	500.2	499.0
5CzBN-OEG	480.4	498.4	509.8	511.0	511.6	516.2	517.2

Table S3. The experimental PLQY values of 5CzBN derivatives doped in PMMA matrix.

Compound	1 wt% PLQY (%)	10 wt% PLQY (%)	30 wt% PLQY (%)	50 wt% PLQY (%)	70 wt% PLQY (%)	90 wt% PLQY (%)	100 wt% PLQY (%)
5CzBN-Eth	67	65	59	49	48	44	41
5CzBN-Pro	67	61	58	53	51	48	43
5CzBN-Hex	67	62	57	55	55	55	55
5CzBN-Hep	68	64	59	57	58	57	57
5CzBN-Non	67	61	62	61	62	60	59
5CzBN-Dod	66	64	65	66	66	65	63
5CzBN-OEG	53	62	55	46	45	42	42

Table S4. The experimental lifetime of 5CzBN derivatives doped in PMMA matrix.

Compound	1 wt% τ_p(ns)/ τ_d (μs)	10 wt% τ_p(ns)/ τ_d (μs)	30 wt% τ_p(ns)/ τ_d (μs)	50 wt% τ_p(ns)/ τ_d (μs)	70 wt% τ_p(ns)/ τ_d (μs)	90 wt% τ_p(ns)/ τ_d (μs)	100 wt% τ_p(ns)/ τ_d (μs)
5CzBN-Eth	36/3.35	47/2.86	40/2.23	33/1.75	34/1.62	28/1.44	30/1.53
5CzBN-Pro	36/3.45	45/3.07	34/2.21	33/1.87	30/1.68	30/1.70	30/1.63
5CzBN-Hex	44/3.68	39/2.73	29/1.93	30/1.75	26/1.68	31/1.70	27/1.59
5CzBN-Hep	36/3.73	34/2.39	33/1.93	30/1.84	33/1.88	34/1.96	35/1.82
5CzBN-Non	46/3.65	35/2.14	34/1.94	33/1.84	30/1.78	24/1.72	32/1.76
5CzBN-Dod	40/3.10	26/1.87	32/1.86	30/1.77	27/1.67	31/1.80	31/1.92
5CzBN-OEG	32/3.86	34/3.08	28/2.40	24/2.05	21/1.84	22/1.82	24/1.77

4. References

[1] a) T. Lu and F. *Chen, J. Comput. Chem*., 2012, **33**, 580-592; b) Z. Liu, T. Lu and Q. Chen, *Carbon,* 2020, **165**, 461-467; c) J. Zhang and T. Lu, *Phys. Chem. Chem. Phys*., 2021, **23**, 20323-20328; d) T. Lu and Q. Chen, *Chemistry-Methods,* 2021, **1**, 231-239.

[2] J. Wang, R. M. Wolf, J. W. Caldwell, P. A. Kollman and D. A. Case, *J. Comput. Chem.,* 2004, **25**, 1157-1174.

[3] M. J. Abraham, T. Murtola, R. Schulz, S. Páll, J. C. Smith, B. Hess and E. Lindahl, *SoftwareX*, 2015, **1-2**, 19-25.

[4] K. Masui, H. Nakanotani and C. Adachi, *Org. Electron*., 2013, **14**, 2721-2726.

[5] G. Zhao, D. Liu, P. Wang, X. Huang, H. Chen, Y. Zhang, D. Zhang, W. Jiang, Y. Sun and L. Duan, *Angew. Chem. Int. Ed*., 2022, **61**, e202212861.